Toward a seasonal precipitation prediction system for West Africa: performance of CFSv2 and high-resolution dynamical downscaling

Jonatan Siegmund, Jan Bliefernicht, Patrick Laux, Harald Kunstmann

Angaben zur Veröffentlichung / Publication details:

Siegmund, Jonatan, Jan Bliefernicht, Patrick Laux, and Harald Kunstmann. 2015. "Toward a seasonal precipitation prediction system for West Africa: performance of CFSv2 and high-resolution dynamical downscaling." *Journal of Geophysical Research: Atmospheres* 120 (15): 7316–39. https://doi.org/10.1002/2014jd022692.

AGU PUBLICATIONS

JGR

Journal of Geophysical Research: Atmospheres

RESEARCH ARTICLE
10.1002/2014JD022692

Key Points:
- Performance of CFSv2 reforecasts for West Africa is intermediate
- Statistical bias correction improves the reforecast quality
- Numerical downscaling can also be a valuable approach

Correspondence to:
J. Siegmund,
jonatan.siegmund@pik-potsdam.de

Citation:
Siegmund, J., J. Bliefernicht, P. Laux, and H. Kunstmann (2015), Toward a seasonal precipitation prediction system for West Africa: Performance of CFSv2 and high-resolution dynamical downscaling, *J. Geophys. Res. Atmos.*, *120*, 7316–7339, doi:10.1002/2014JD022692.

Received 22 OCT 2014
Accepted 14 JUN 2015
Accepted article online 18 Jun 2015
Published online 4 AUG 2015

Toward a seasonal precipitation prediction system for West Africa: Performance of CFSv2 and high-resolution dynamical downscaling

Jonatan Siegmund[1,2], Jan Bliefernicht[2], Patrick Laux[1], and Harald Kunstmann[1,2]

[1] Institute of Meteorology and Climate Research, Atmospheric Environmental Research (IMK-IFU), Karlsruhe Institute of Technology, Garmisch-Partenkirchen, Germany, [2] Chair for Regional Climate and Hydrology, University of Augsburg, Augsburg, Germany

Abstract Seasonal precipitation forecasts are important sources of information for early drought and famine warnings in West Africa. This study presents an assessment of the monthly precipitation forecast of the Climate Forecast System version 2 (CFSv2) for three agroecological zones (Sudan-Sahel, Sudan, and Guinean zone) of the Volta Basin. The CFSv2 performance is evaluated for the Sahel drought 1983 and for all August months of the reforecast period (1982–2009) with lead times up to 8 months using a quantile-quantile transformation for bias correction. In addition, an operational experiment is performed for the rainy season 2013 to analyze the performance of a dynamical downscaling approach for this region. Twenty-two CFSv2 ensemble members initialized in February 2013 are transferred to a resolution of 10 km × 10 km using the Weather and Research Forecasting (WRF) model. Since the uncorrected CFSv2 precipitation forecasts are characterized by a high uncertainty (up to 175% of the observed variability), the quantile-quantile transformation can clearly reduce this overestimation with the potential to provide skillful and valuable early warnings of precipitation deficits and excess up to 6 months in ahead, particularly for the Sudan-Sahel zone. The operational experiment illustrates that CFSv2-WRF can reduce the CFSv2 uncertainty (up to 69%) for monthly precipitation and the onset of the rainy season but has still strong deficits regarding the northward progression of the rain belt. Further studies are necessary for a more robust assessment of the techniques applied in this study to confirm these promising outcomes.

1. Introduction

Numerical weather forecasts allow to predict weather conditions up to 10 days in advance. Longer forecasting periods, however, are highly desirable for many purposes such as agricultural production, water supply and distribution management, and prevention and preparation for weather-related humanitarian disasters. Reliable seasonal precipitation forecasts are important especially for subtropical/tropical water-limited regions, where precipitation deficits during the rainy season heavily affect large parts of the population, most of them living indirectly or directly from rainfed agriculture. In those regions the monsoon rain is the crucial source of precipitation. West Africa, the area of interest in this study, is affected by an intensive intraseasonal, interannual, and interdecadal rainfall variability [*Nicholson*, 2001; *Schneider et al.*, 2011] causing large-scale and long-lasting droughts in the past, such as the Sahel droughts in the beginning of the 1980s. Agriculture in West Africa is highly vulnerable to subnormal precipitation amounts, since large parts of its agriculture relies on rainfed crop production [*Wani et al.*, 2009]. Knowing the variability of monsoonal rains in advance may contribute to prevent crop failures which could finally help to stabilize or even increase the level of food security.

Since the end of the 1990s, precipitation forecasts for the upcoming rainy season in West Africa are operationally performed within the framework of PRESAO (Prévisions Saisonniéres en Afrique de l'Ouest). PRESAO is a joint initiative of the African Centre of Meteorological Applications for Development (ACMAD), the national weather services of the West African countries, and several international weather and climate research institutions (for further information, see www.acmad.net). The current seasonal PRESAO forecast product is a map for the seasonal precipitation amount from June to August, highlighting those regions in West Africa with

expected deficit or excess in precipitation. The forecast product is based on the analysis of several sources of information, e.g., the latest forecast information of global seasonal ensemble prediction systems (GSEPS) such as the Climate Forecast System (CFS) from National Centers for Environmental Prediction (NCEP) [*Saha et al.*, 2006, 2013] and the precipitation forecasts of the national weather services for their region of interest based on statistical techniques which use sea surface temperature observations and predicted atmospheric information from GSEPS. In a final step, the individual information is merged and reinterpreted by the group of meteorologists to formulate a harmonized precipitation forecast for West Africa. The main advantage of PRESAOs seasonal precipitation forecasts is the usage of various sources of information and forecasting techniques in combination with meteorological expert knowledge. The reliability of the seasonal PRESAO forecasts has been analyzed by few studies only. In a report by *Mason and Chidzambwa* [2009], e.g., PRESAOs reliability has been found to be reasonable. However, the current operational practice of PRESAO also has shortcomings:

1. The premonsoonal and postmonsoonal periods are not covered by the forecasts, yet these periods are very important for agricultural considerations.
2. The current forecasts provide the total precipitation sum of a 3 month period, but the weather information is needed at a much higher temporal resolution. The relevance of the 3 month sums for smallholders in the tropics is questionable as several rainfall characteristics on smaller time scales are needed [*Hansen et al.*, 2011; *Moron et al.*, 2013].
3. Agriculturally relevant intraseasonal precipitation characteristics, such as the date of the onset of the rainy season or the length of intraseasonal dry spells, are not provided by the current procedure yet are highly desired by local stakeholders in agriculture [*Roncoli et al.*, 2002].
4. The lead time is limited to 1 month. But an extension of the forecasts' lead time would expand the range of options for preventive actions that allow to cope with extreme events like droughts.

In order to deal with these shortcomings, GSEPS can be a first source of information for providing regional precipitation forecasts for West Africa. Several international weather institutions run their own GSEPS to provide forecasts for precipitation and other variables with lead times of 6 months and more. Prominent GSEPS are the CFS of NCEP and the global EPS of the European Centre for Medium-Range Weather Forecast (ECMWF) [*Stockdale et al.*, 2011]. One of the earliest studies showing that real-time temperature and precipitation forecast of GSEPS can be skillful for many geographical regions was performed by *Wilks and Godfrey* [2002]. *Ndiaye et al.* [2011] furthermore found promising results of GSEPS forecasts for the West African Sahel region.

The integral part of these systems is a coupled oceanic-atmospheric general circulation model. The latest generation of these models, the CFS version 2 (CFSv2) and the fourth generation of the global EPS of ECMWF, became operational in 2011 [*Saha et al.*, 2013; *ECMWF*, 2014]. These systems include a set of reforecasts, providing the possibility to investigate the system's predictive skill over a long time period. ECMWF's seasonal forecasting products have been analyzed and used for applications in Africa, e.g., by *Dutra et al.* [2013a, 2013b], *Di Giuseppe et al.* [2013], or *Mwangi et al.* [2014]. Recently, *Sheffield et al.* [2014] developed a drought monitoring and forecasting system, using downscaled CFSv2 seasonal temperature and precipitation predictions in combination with hydrological modeling and remote sensing approaches. The CFSv2 reforecasting skill has systematically been analyzed for various geographical regions of the world, focusing on sea surface temperature (SST), precipitation, and further variables. For instance, *Hu et al.* [2012] and *Xue et al.* [2013] analyzed CFSv2's reforecasting potential for North Atlantic and global tropical SST, respectively.

The West African rainfall regime is only weakly triggered by El Niño–Southern Oscillation variations. This is one of the reasons dynamically driven long-time precipitation forecasts only exhibit intermediate forecasting skills for this region, so far [e.g., *Yuan et al.*, 2011; *Dutra et al.*, 2013b]. For instance, *Yuan et al.* [2011] found a low predictive skill for precipitation over West Africa for lead times higher than 1 month. Even for the 1984 Sahel drought patterns, the CFSv2 reforecast with a lead time of 4 months only had shown very low correlation with the reanalysis data. *Zuo et al.* [2013] analyzed CFSv2's reforecasting skill for monsoonal precipitation and tropical SST for Southeast Asia, Equatorial Africa, and Central America. The prediction of monsoonal precipitation was found to be skillful for America and Asia up to 5 months in advance, while the predictive skill was comparatively low for the African monsoon probably due to the low model performance of predicting the tropical Atlantic SST. Monsoonal rainfall in West Africa is on the large scale forced by an interplay of atmospheric and oceanic circulation patterns, e.g., nearby Atlantic sea surface temperatures and the current Atlantic Meridional Overturning Circulation (AMOC) situation [e.g., *Fontaine and Janicot*, 1996; *Shanahan et al.*, 2009]. A detailed overview of the large-scale driving factors is given by *Nicholson* [2013].

On the regional scale, precipitation patterns are additionally modified by the land surface conditions [e.g., *Steiner et al.*, 2009; *Kunstmann and Jung*, 2007]. The combination of these factors modulates timing, strength, and positioning of the West African monsoon.

Real-time forecasts of global EPS can be accessed for many atmospheric variables via operational archives. The type of variables, the temporal resolution, and the lead time of the available forecast information is sufficient for many real-time applications. However, a crucial shortcoming remains the coarse spatial resolution of global forecasts. A specific application highlighting this problem for hydrological applications in West Africa was presented by *Lebel et al.* [2000]. It is therefore common in weather forecasting and climate projections to transfer large-scale general circulation model (GCM) information to the geographical region of interest by using statistical or dynamical downscaling approaches. A common approach in dynamical downscaling is to nest an atmospheric model in a GCM, simulating the atmospheric flow for a limited geographical region. One of the earliest applications for West Africa was performed by *Jenkins* [1997]. Since then, many further dynamical downscaling approaches have been performed for this region [e.g., *Jung and Kunstmann*, 2007; *Sylla et al.*, 2011]. Recently, the CFSv2 reforecasts have been tested for dynamical downscaling purposes yet not for West Africa. For instance, *Huang and Chan* [2013] used RegCM3 for tropical cyclone genesis over the western North Pacific. The reforecasting of cyclone landfall frequency and locations could be slightly improved by the dynamical downscaling approach. Statistical approaches are used to improve the precipitation forecast of GCMs for West Africa [e.g., *Ndiaye et al.*, 2009]. An overview of statistical and dynamical downscaling approaches for West Africa is given by *Paeth et al.* [2011]. Recently, *Yuan et al.* [2013b] presented a study to establish a hydrological drought forecasting system for Africa based on CFSv2. The meteorological forecasts of CFSv2 are refined by statistical approaches and used as input information for a land surface model.

The novelty of this study is two sided: First, an evaluation of the CFSv2 reforecast performance for monthly precipitation amounts in August is performed for the entire reforecast period and for lead times up to 8 months with a special focus on the severe Sahel drought 1983. In contrast to former studies performed for this region, e.g., *Yuan et al.* [2013a] or *Zuo et al.* [2013], this study analyzes the raw and corrected CFSv2 monthly precipitation amounts. The correction of the CFSv2 precipitation forecasts is performed using a quantile-quantile transformation similar to *Themeßl et al.* [2011] but applying this approach for ensemble forecast and for monthly precipitation for eliminating systematic differences between forecasts and observations. The corresponding performance of the corrected and raw CFSv2 forecasts is evaluated in the physical and probability space using standard metrics often applied in an operational forecasting for two important forecast attributes: Forecast accuracy and forecast uncertainty. The latter attribute tends to receive only little attention in many studies. In this study, we construct a novel relative measure which relates the uncertainty of the CFSv2 forecasts to the observational uncertainty.

Second, the conduction of a seasonal forecasting experiment is performed, using a dynamical downscaling approach to provide a regional ensemble forecast consisting of 22 members for the rainy season 2013 in West Africa. The Weather and Research Forecasting (WRF) model is applied using the real-time ensemble forecasts of CFSv2. WRF has been recently tested for this region in a reanalysis framework by *Klein et al.* [2015] focusing on the model's ability to represent dominant large-scale atmospheric patterns that drive the West African monsoon. The performance of this regional ensemble prediction system is analyzed for standard variables in seasonal forecasting such as the monthly precipitation amount. Additionally, an intraseasonal daily rainfall characteristic, the date of the onset of the rainy season, is analyzed. Those intraseasonal characteristics are needed to improve the current operational practices in West Africa. The performance of our approach is investigated in comparison to the raw CFSv2 forecasts, a low-skill reference forecast, and two observational monitoring products. In addition, this study gives first insights whether the usage of raw, statistically corrected or dynamically downscaled CFSv2 forecasts is worth to be used as an additional source of information for the PRESAO seasonal outlooks.

2. Study Area and Data

2.1. Description of the Study Area

The area of interest in this study (Figure 1) is West Africa with a focus on the Volta Basin. Spanning six countries, the Volta Basin ranges over various climatic and ecologic regimes. For the analyses the Volta Basin is subdivided into three agroecological zones: the *Sudan-Sahel zone* north of 11°N, the *Sudan zone* between 11°N and 8.5°N referring to *Barry et al.* [2005], and the *Guinea Coast* south of 8.5°N referring to *Sylla et al.* [2009]. In Figure 2 the monthly areal precipitation amounts for the three agroecological zones are illustrated.

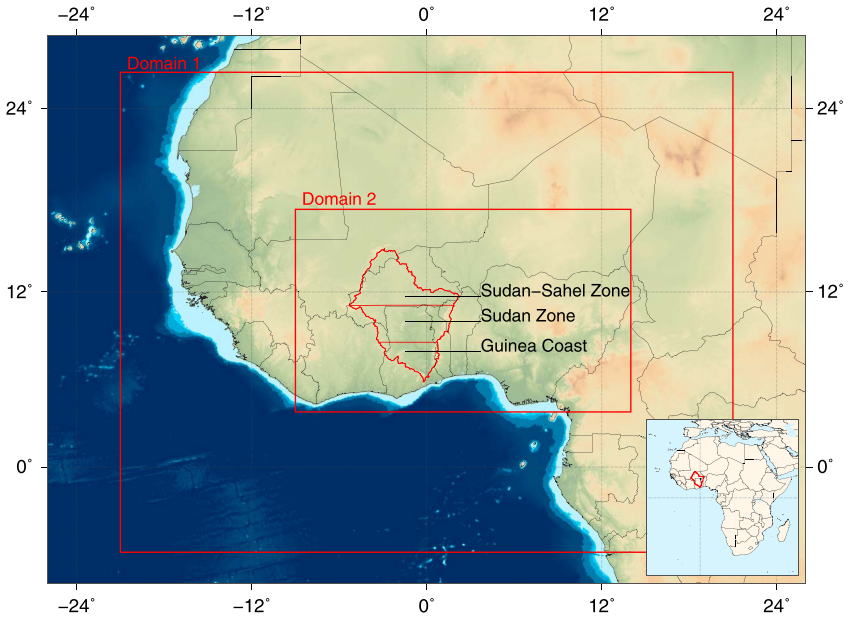

Figure 1. The Volta Basin in West Africa and the agroecological zones for which the analyses are performed and the domains used for dynamical downscaling (spatial resolution of Domain 1 (Domain 2) is 30 km × 30 km (10 km × 10 km)). Land and sea color signatures indicate the elevation level.

The northern zones are characterized by one rainy season with a peak during July and August, while the precipitation regime of the Guinean Coast zone is characterized by two rainy seasons per year with peaks in May/June and in September. The shaded areas in Figure 2 show the interannual rainfall variability, indicated by the range between the 10th and 90th percentiles of the period from 1971 to 2010. Additionally, the monthly areal precipitation of the extreme dry year 1983 is highlighted in Figure 2. The monthly precipitation amount of 1983 is characterized by strong negative deviations from the climatological mean, in particular from July to September for the Guinean Coast and the Sudan zone.

In addition to that, Figure 3 illustrates the northward propagation of the rain belt over West Africa during the summer rainy season. As known from *Nicholson* [2009], this rain belt does not represent the location of the land Intertropical Convergence Zone (ITCZ) but is a result from uprising air in between the African Easterly Jet and the Tropical Easterly Jet. In addition, a very specific rainfall characteristic of southern West Africa in the midsummer dry period between July and August is illustrated in Figure 3, ranging from Côte d'Ivoire to Nigeria along the Guinean coastline. This summer drop in rainfall is also mirrored by the local vegetation: In the area around the coastal regions of Ghana, Togo, and Benin the rain forest is interrupted by a savanna corridor, the so called Dahomey Gap [*Salzmann and Hoelzmann*, 2005].

2.2. Reforecasts and Real-Time Forecasts of the Climate Forecast System Version 2

The provided CFSv2 data consist of three products, the CFS reanalysis (CFSR), the CFSv2 reforecasts, and the CFSv2 real-time forecasts. In this study we use the 28 years (1982–2009) set of CFSv2 reforecasts and the real-time forecasts of February 2013 which are briefly described in the following sections.

2.2.1. CFSv2 Reforecasts

The CFSv2 reforecasts have the advantage that the performance of a forecasting technique can be tested for many years. For every month during the time period from 1982 to 2009, 20–28 reforecasts over a time period of 9 months are available. Additionally, several reforecasts with shorter lead times (3 months and 45 days) are provided for the period 1999–2009. The temporal resolution of the data is 6 h with a spatial resolution of 1° [*Saha et al.*, 2013; *Saha and Tripp*, 2013]. These reforecast data are available for selected atmospheric variables at various pressure levels provided by *NOAA* [2014]. In this study we use the monthly precipitation data of the 9 months forecast runs to analyze the CFSv2 performance. Due to the large data amount, not all pressure levels of the forecast runs are archived by *NOAA* [2014]. Thus, only a very limited number of pressure levels would be available as input information for dynamical downscalings. To overcome this problem, we use CFSv2 real-time forecasts.

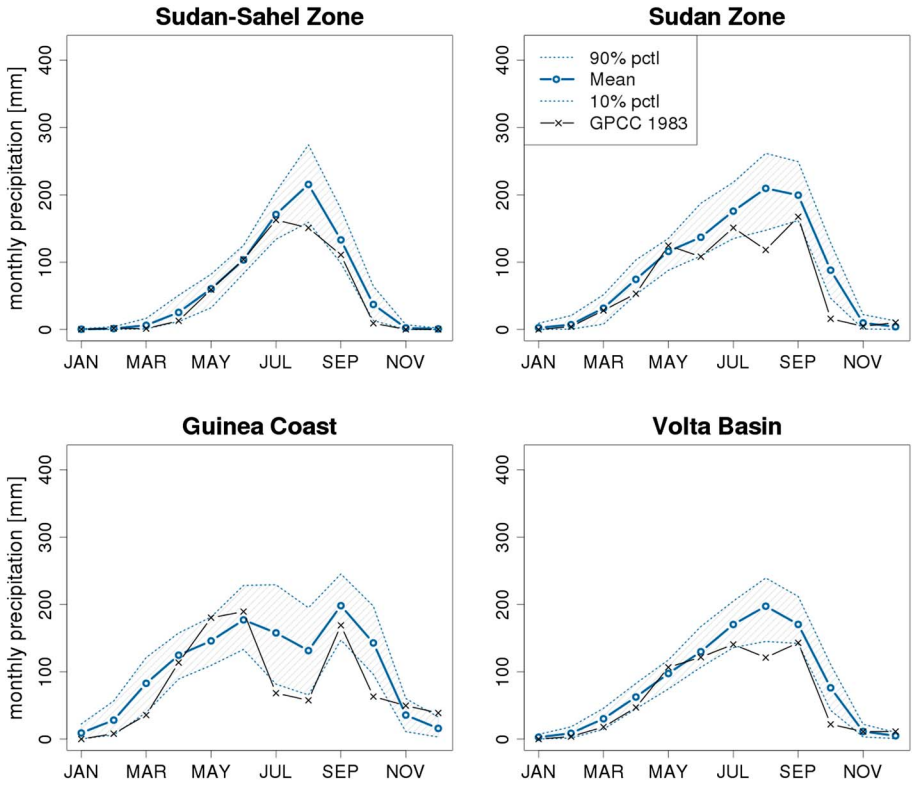

Figure 2. Mean monthly areal rainfall and rainfall variability for the three agroecological zones and the Volta Basin itself taken from GPCC reanalysis (1971–2010). Percentiles refer to all observations of the 40 year period from 1971 to 2010. In addition, the mean monthly areal rainfall amount of 1983 is illustrated.

2.2.2. CFSv2 Real-Time Forecasts

The CFSv2 operational forecasts continue the CFSv2 reforecasts, operationally providing real-time forecasts with three different lead times. Every day four 9 months runs are initialized at 0, 6, 12, and 18 UTC. In addition, three 3 month runs are initialized at 0 UTC, and three 45 days runs (nine per day) are initialized at 6, 12, and 18 UTC. The operational CFSv2 data are provided in 6-hourly resolution for all variables needed to drive WRF [*Skamarock et al.*, 2008]. For the downscaling we use temperature, *u* wind and *v* wind components, relative humidity, and geopotential height at 28 pressure levels. Additionally, sea level pressure and surface pressure are used. The sea surface temperature information is substituted by the skin temperature in order to overcome the problem of missing sea surface temperature data along the shoreline.

The CFSv2 real-time forecasts runs of the last 7 days are available by a 7 days rotating archive at *NOAA* [2014]. While CFSR provided the initial conditions for the reforecasts, the Climate Data Assimilations System (CDAS by NCEP/National Center for Atmospheric Research) provides the initial conditions for the operational CFSv2 forecasts. CDAS is the operational continuation of CFSR. This is why the data assimilation for the CFSv2 operational forecasts has a resolution of T574 (at equator $\approx$ 34 km) instead of T382 (at equator $\approx$ 52 km) as for the CFSv2 reforecasts. This is one of the key differences between the reforecasts and the real-time forecasts of CFSv2 [*Saha et al.*, 2013; *NCEP*, 2013].

2.3. Observational Data

To compare the precipitation forecasts of the global CFSv2 and the regional CFSv2-WRF with measurements, we use different observational data sets. These are globally gridded gauge measurements (Global Precipitation Climatology Centre, GPCC) and gauge-corrected satellite data (RFE2).

2.3.1. GPCC

The Global Precipitation Climatology Centre (GPCC) data sets provided by the German Weather Service are globally gridded monthly land surface precipitation amounts. In this study the GPCC Full Data Reanalysis version 6.0 [*Schneider et al.*, 2011] with a resolution of 0.5° available from 1971 to 2010 is used. In addition,

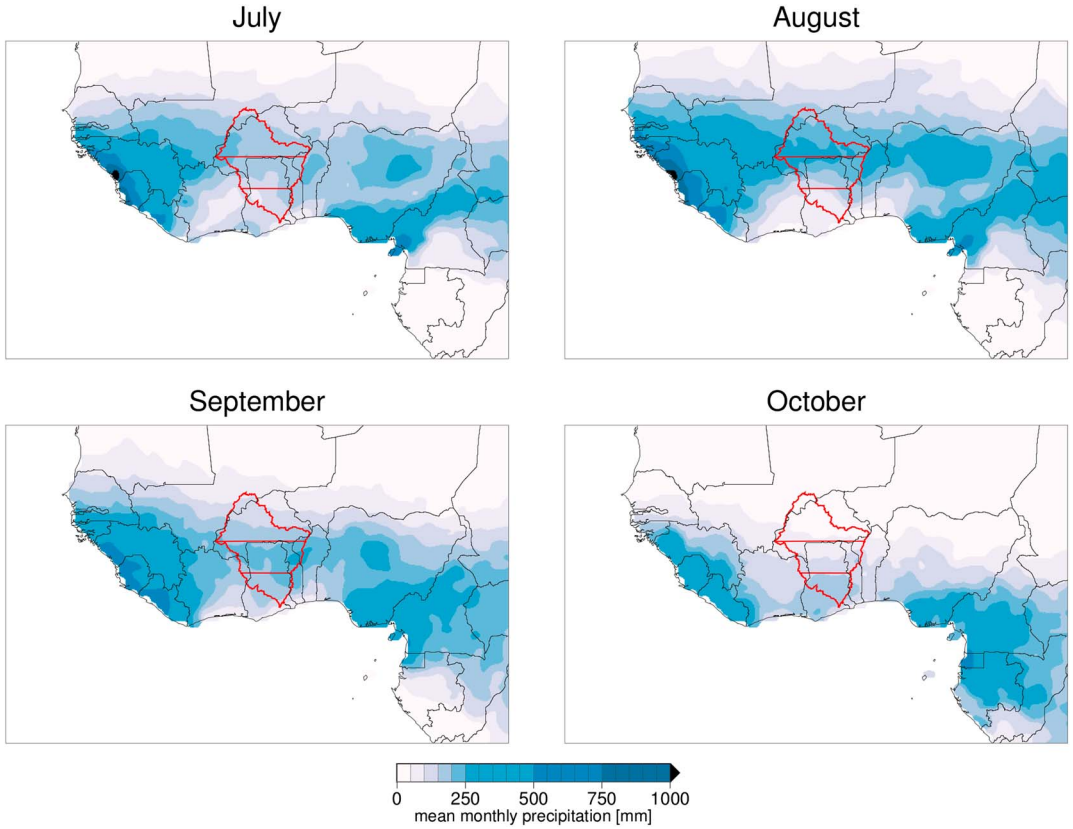

Figure 3. Mean monthly rainfall over West Africa for the central months of the summer monsoon from GPCC reanalysis (1971 – 2010).

we use the monthly precipitation amounts of Near Real-Time First Guess Monthly Land-Surface Precipitation [*Ziese et al.*, 2011], available at a resolution of 1° from 2005 until today. The GPCC data sets are pure gauge measurements, interpolated to a regular grid for global land surfaces.

A generally critical aspect, which has to be considered when comparing model data to gridded precipitation data sets, is the data set's gauge station density in the study area. For the GPCC reanalysis this has been globally analyzed by *Lorenz and Kunstmann* [2012]. In West Africa, as well as in most other parts of the world, the number of gauges used for GPCC has been continuously decreasing during the last decades. While the gauge station density in the study area is comparatively high for the 1980s, it is quite low for the years after 2000.

2.3.2. RFE2

African Rainfall Estimate version 2 (RFE2) [*NOAA CPC*, 2013] is a combined satellite-gauge data product, operationally provided by the Climate Prediction Center, National Weather Service of the United States of America (CPC), and is part of the Famine Early Warning System Network. The spatial resolution is 0.1°, available for the entire African continent in the time period from 2001 until today. The rainfall estimates in RFE2 are derived from three satellite data sets and are merged by a maximum likelihood estimation. Finally, the data are fitted to the Global Telecommunication System (World Meteorological Organization Global Telecommunication System) gauge measurements [*NOAA CPC*, 2013]. The RFE2 data are used for the comparison with the real-time forecasts because of its high temporal and spatial resolution, making RFE2 preferable against other monitoring products. A further advantage is the fast data availability with a latency of only 6 h.

3. Methodology

3.1. Statistical Correction of the CFSv2 Precipitation Forecasts

Prior to the analyses of the CFSv2's reforecast performance, we apply a normal-quantile transform [see *Themeßl et al.*, 2011; *Bogner et al.*, 2012; *Krzysztofowicz*, 1997] to the raw CFSv2 data, in order to remove the systematic differences between forecasts and observations. This technique is a frequently used correction method for eliminating systematic differences. *Themeßl et al.* [2011] used this approach for the correction of

daily precipitation amounts obtained from a regional climate model and illustrated that the approach is superior in combination with further statistical downscaling techniques. *Bardossy and Pegram* [2011] refined this methodology by introducing weather patterns into the correction algorithms. They applied this approach for areal averaged daily precipitation amounts from a regional climate model. In our approach we follow the work of *Themeßl et al.* [2011] but our correction algorithm is applied for monthly areal precipitation amounts, similar to the fashion of *Bardossy and Pegram* [2011], but for each month of the year, each lead time and region separately. The following steps are performed:

1. Sort all observations $x = \{x_1, x_2, ..., x_n\}$ of a given region for all August months of the selected time period (1971–2010) from smallest to largest value and determine ranks R_{x_i} for each observation x_i, where $i = 1, 2, ..., n$ and n = number of observations.
2. Determine an empirical cumulative distribution function of the observations F_x by calculating cumulative frequencies p_i for each observation using the plotting position formula $p_i = R_{x_i}/(n+1)$.
3. Sort all reforecast ensemble members $y = \{y_1, y_2, ..., y_m\}$ from all ensembles with the same lead time (1982–2009) from smallest to largest and determine ranks R_{y_i} for each forecast value y_i, where $i = 1, 2, ..., m$ and m = number of reforecasts.
4. Determine empirical cumulative distribution function F_y by calculating cumulative frequencies q_i using the same plotting position formula $q_i = \frac{R_{y_i}}{(m+1)}$.
5. Determine corrected forecast value y_i' for each q_i by using the inverse cumulative distribution function of the observations $y_i' = F_x^{-1}(q_i)$.
6. Repeat steps 3 to 5 for each lead time.

We use the GPCC reanalysis as reference climatology for the correction of CFSv2 precipitation and apply the transformation for monthly mean areal precipitation.

3.2. Statistical Verification of the CFSv2's Precipitation Reforecasts

In a first step, a verification of the CFSv2 reforecast performance for the monthly areal precipitation amount is performed for the Sahel drought 1983. The target month of this investigation is August 1983 where very unusual low-precipitation amounts have been observed. In order to investigate whether CFSv2 would have forecasted this event 6 months in advance if it had been operational at that time, the CFSv2 reforecast runs with a duration of 9 months, initialized in February 1983, are used for this analysis. In addition, this analysis is repeated for shorter (1 to 5 months) and longer lead times (7–8 months) using CFSv2 reforecast ensembles initialized from November 1982 to July 1983 in order to analyze how the ensemble spread (forecast uncertainty) and the forecast accuracy are evolving related to the lead time. As reference data for these analyses, the GPCC reanalysis observations are used.

In a second step, a verification of the CFSv2 reforecasts is performed for monthly areal precipitation amounts of the August months of the entire retrospective forecast period from 1982 to 2009. To estimate the uncertainty of the reforecasts, the interdecile range (IDR_y) of the ensemble forecast is calculated. The IDR_y is the difference between the 10th and the 90th percentiles of the members of an ensemble forecast. Thus, the IDR_y ranges between 0 mm and infinity; low values indicate a small uncertainty. We calculate the CFSv2 reforecast IDR_y for the target month August and various lead times (τ). A desirable characteristic of a (re)forecast system is a small forecast uncertainty compared to the observational uncertainty. To construct a relative measure which can quantify this relationship, the IDR of CFSv2 reforecasts is divided by the IDR of the climatological distribution of the observations (IDR_x), resulting in a relative interdecile range (RIDR). The IDR_x is the difference between the 10th and the 90th percentiles of the GPCC August observations for the analyzed period:

$$\mathrm{RIDR}(\tau) = \frac{\mathrm{IDR}_y(\tau)}{\mathrm{IDR}_x} \tag{1}$$

The RIDR can range between 0 and infinity. If RIDR is smaller than 1, the CFSv2 forecast uncertainty (width of the ensemble spread) is smaller than the observed variability based on the past GPCC observations. If RIDR is 1, the forecast uncertainty is identical to the observational uncertainty.

To quantify the forecast accuracy, we calculate the relative mean absolute differences (RMADs) between reforecasts and observations for various lead times (pertaining August):

$$\mathrm{RMAD}(\tau) = \frac{\frac{1}{n}\sum_{i=1}^{n} |x_i - \bar{y}_i(\tau)|}{\bar{x}} \cdot 100\% \tag{2}$$

where x_i is the observed monthly areal precipitation (here for August) in the ith year; y_i is the arithmetic mean of the CFSv2 ensemble (here for August) in the ith year; n is the number of joint reforecast and observation pairs; and $\bar{x}$ is the observed climatological mean (GPCC) of the monthly areal precipitation (here for August) calculated from GPCC reanalysis data. The RMAD ranges between 0% and positive infinity where a low value indicates a high accuracy. A forecast with a RMAD of zero is identical to the GPCC observations.

The RMAD and the RIDR are selected to evaluate the corrected and raw CFSv2 precipitation forecasts in the physical space. The major reason is that corrected GSEPS precipitation forecasts (using statistical approaches) are also used for subsequent applications like drought forecasting. The corrected GSEPS precipitation is usually the main input information for distributed land surface models or hydrological models. In this case the absolute values of the corrected CFSv2 forecasts are of interest, as well, and corresponding verification measures can give some valuable insight regarding the performance of a selected forecasting technique in the physical space. In addition, we calculate the ranked probability score RPS_y to determine the accuracy of CFSv2 forecasts in the probability space. The ranked probability score was proposed by *Epstein* [1969], and it is one of the most frequently used scores to determine the quality of probabilistic forecasts. Detailed information regarding the calculation of this measure is given by *Wilks* [2011]. In this study the forecast probabilities are determined for three precipitation categories based on the terciles. The categorization is identical to the frequently applied three categories ("below average," "climatology," and "above average") in seasonal forecasting [*Wilks and Godfrey*, 2002] which are based on terciles. These precipitation categories are also used in PRESAO [*Mason and Chidzambwa*, 2009]. We also calculate the ranked probability score RPS_x using the climatological forecasts to compare the accuracy of the CFSv2 precipitation forecast (corrected and raw) in comparison to a low-skill reference forecast. The same precipitation categories are used for a calculation of the RPS_x using the GPCC observations. If RPS_y is smaller (greater) than RPS_x, the accuracy of the CFSv2 forecast is better (worse) in comparison to the climatological forecast. They are identical if $RPS_y = RPS_x$.

The evaluation using the areal precipitation amount for a given region is similar to the work presented by *Bardossy and Pegram* [2011] who corrected the gridded RCM precipitation output with gridded observed precipitation based on a quantile-quantile transformation. In our approach, we aggregated the monthly CFSv2 and GPCC precipitation fields directly to the scale of the agroecological zones. The primary reason is the sparse precipitation network in West Africa in particular within the last 20 years [e.g., *Lorenz and Kunstmann*, 2012] which have been used for the generation of global precipitation products such as GPCC. The aggregation is performed to obtain a better estimate for the observed areal precipitation. In this case the estimation of the areal precipitation is based on a higher number of observations in comparison to an evaluation on a finer spatial scale.

Probabilistic skill scores are often very low, in particular for precipitation extremes, hiding the real value of a forecast system although the accuracy in terms of a probabilistic binary warning system can be very high. This problem is illustrated by, e.g., *Jolliffe and Stephenson* [2012] or *Bliefernicht* [2011]. To overcome this problem, we determine hit rate and false alarm rate to evaluate the CFSv2 precipitation forecasts in terms of a binary warning system. The hit rate H and false alarm rate F are calculated for both terciles based on a set of 20 probability thresholds used for a warning to determine the curves of the relative operating characteristics (ROC diagram) [e.g., *Hogan and Mason*, 2012]. A positive skill is indicated when the hit rate is larger than the false alarm rate ($H > F$). Based on this information, we also calculate the Peirce skill score PSS which is the hit rate minus the false alarm rate [e.g., *Hogan and Mason*, 2012] $PSS = H - F$. In comparison to other common binary skill measures, the PSS has the property that it can be used to assess the value of the forecast information, one of the most important forecast attributes in weather forecasting or in climate prediction. The Peirce skill score is identical to the maximum economic value of a forecast system [*Richardson*, 2003]. The economic value is a measure to address the utility of a warning system in terms of monetary costs. The number of alarms of a warning system is related to alarm costs due to protective action and the corresponding number of misses to monetary losses. To determine the benefit of a warning system, the total expense (sum of alarm costs and monetary losses) of the warning system is compared to the optimum total expense of a warning system that produces no warning (no protection) or always a warning (total protection).

3.3. Dynamical Downscaling of CFSv2 Real-Time Forecasts Using WRF

In order to investigate the benefit of a dynamical downscaling of the CFSv2 forecasts, the operational forecasts for 2013 are downscaled for the Volta Basin to a resolution of 10 km × 10 km using WRF-ARW version 3.4.1 [*Skamarock et al.*, 2008]. The operational simulation experiment is performed using 22 members of the CFSv2

forecast runs initialized in February 2013 to cover the most important time of the rainy season in West Africa (June, July, and August) with a sufficient lead time. This technique has the additional advantage that the pre-monsoon period from March to May is covered. This period is needed to forecast the date of the onset of the rainy season. Since CFSv2 provides a number of forecasts with lead times less than 3 months, only those simulation runs with a lead time of 9 months can be used for this experiment. The total number of these forecast runs is still very large ($n = 112$ for February 2013) because four 9 months simulation runs are initialized every day. To reduce the computational amount for the downscaling experiment and to create an ensemble with a large range of different initiation times, only one CFSv2 simulation per day is selected for the downscaling experiment ensemble. Due to missing time steps in the provided CFSv2 data, not all of the 28 CFSv2 February simulation runs are used. Finally, the experiment uses a time-lagged ensemble consisting of one 0 UTC simulation run of almost each day in February 2013. The CFSv2 input data are available in 38 vertical levels and 6-hourly temporal resolution.

The downscaling is conducted until 31 August 2013 using two one-way nesting domains (Figure 1). The horizontal resolution of the inner domain is 10 km. In both domains we use 28 atmospheric levels with an atmospheric top at 5000 Pa with an adaptive time step for numerical integration. The high model top is chosen in order to be able to represent the very high altitude of the tropopause, as it is typical for tropical regions like the study area. The combination of a comparably low vertical resolution with a high model top has formerly been used in, e.g., *Jung and Kunstmann* [2007] for this region. The WRF model is nested in the CFSv2 based on conventional sponge technique where the atmospheric forcing is purely determined from the boundary conditions. Beside this technique, there are several further approaches such as the spectral nudging [e.g., *von Storch et al.*, 2000]. An overview about various alternative nesting approaches is given in, e.g., *Liu et al.* [2014].

We also performed a comprehensive analysis in a reanalysis framework using WRF and ERA-Interim data regarding the ability to represent large-scale atmospheric features that drive the West African monsoon. The results of these experiments are summarized in *Klein et al.* [2015]. The selected parameterization schemes and further model setup such as the vertical resolution used in the ensemble experiment are based on experiences from former studies made for this region using MM5 [*Jung and Kunstmann*, 2007] and using WRF to downscale ERA-Interim and CFSR reanalysis data for the wet seasons 1999 and 2002 [*Bliefernicht et al.*, 2013]. For the microphysics we use the *WRF single-moment 3-class scheme* [*Hong et al.*, 2004]; the longwave radiation is calculated by a *Rapid Radiative Transfer Model* based on *Mlawer et al.* [1997], while the *Dudhia scheme* [*Dudhia*, 1989] is used for the shortwave radiation. The land surface physics are computed by the *Noah Land Surface Model* [*Tewari et al.*, 2004], and the planetary boundary layer is treated by the *Yonsei University scheme* [*Hong et al.*, 2006]. As cumulus scheme we use the *Betts-Miller-Janjic scheme* [*Janjic*, 1994], and CFSv2 soil moisture is used for land surface initialization. A distinct model spin-up time is not considered, because the time between the initialization in February and the monsoonal rainfalls between June and September can be expected to be sufficient for the regional model to build up the relevant atmospheric circulation features.

3.4. Calculation of Intraseasonal Rainfall Characteristics

The definition of ORS (onset of the rainy season) applied in this study is based on an agricultural approach to recommend planting time following *Laux et al.* [2008]. The method has already been applied for the Volta Basin in West Africa [*Laux et al.*, 2008, 2009] and further improved for Cameroon [*Laux et al.*, 2010]. The ORS is defined as the first day of a wet spell with significant rainfall amounts for cropping and without any crop damaging dry spell within the month afterward. In this approach, these criteria are translated into the following three fuzzy rules: (1) at least 25 mm total precipitation within five consecutive days. (2) This period is characterized by a wet starting day (wet = min 2 mm/d) and at least two further wet days in that period. (3) No dry spell longer than 6 days during the next 30 days. Since the WRF and CFSv2 produce multiple "drizzle" events, the ORS approach used in this study is slightly modified by an empirical 2 mm threshold, transferring all daily precipitation amounts smaller than 2 mm into 0 mm. Otherwise, the drizzle results in unrealistic early ORS dates.

4. Results

4.1. Statistical Analyses of CFSv2 Reforecasts for Monthly Areal Precipitation

Figure 4 shows the comparison of a corrected CFSv2 6 months lead time reforecast ensemble to the GPCC observations for the rainy season 1983 across the Volta Basin. In addition, the raw CFSv2 precipitation forecasts are shown in the background. The statistical correction can clearly reduce the ensemble spread of the

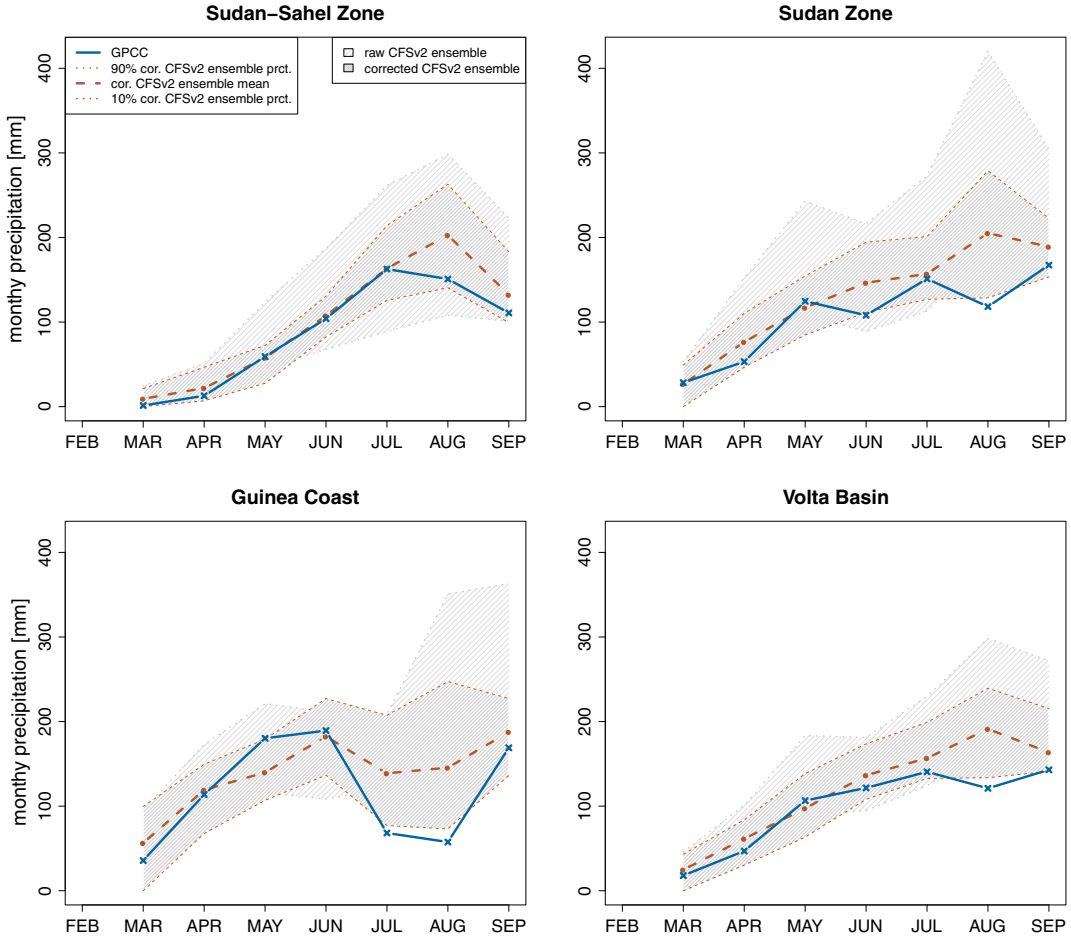

Figure 4. Bias-corrected and raw CFSv2 reforecast for monthly areal precipitation for the major drought event 1983, ensemble (20 runs) initialized in February. As all ensemble members start from different days in February, the entire ensemble forecast starts in March.

CFSv2 precipitation forecast reducing the CFSv2 forecast uncertainty. For the Sudan-Sahel zone the ensemble mean of the corrected reforecast is very close to the observed areal precipitation from March to July. Yet the ensemble mean overpredicts the observed precipitation during August and September. Although all observations are within the ensemble spread, the comparison of the CFSv2 reforecast with the observed variability (Figure 2) illustrates shortcomings for this event, even for the corrected CFSv2 forecast. The uncertainty of the corrected precipitation forecast is very large especially during July, August, and September, and the severe drought in August is not indicated by many CFSv2 ensemble members. For the Sudan zone, the ensemble mean of the corrected CFSv2 forecasts overpredicts the areal precipitation amounts during most of the months of the investigation period in particular for August. The observations in August are even lower than the ensemble's 10th percentile. The unusually dry conditions during July and August at the Guinea Coast are also not indicated by the corrected CFSv2 ensemble mean. The observations are even lower than the 10th ensemble percentile.

Averaged over all zones and months (March – September), the corrected CFSv2 ensemble spread is in a similar range (IDR_y of 1983 = 79 mm) like the observed variability (IDR_x of 1983 = 77 mm). Although the CFSv2 is characterized by a high forecast uncertainty, the ensemble spread is not able to cover all observations, in particular for those months which are extremely dry.

The ensemble means and ensemble spreads of eight uncorrected and corrected CFSv2 ensembles with lead times of 1 – 8 months pertaining August 1983 in comparison to the observed August precipitations for all zones are illustrated in Figure 5. Corrected and uncorrected CFSv2 reforecasts overestimate the observed

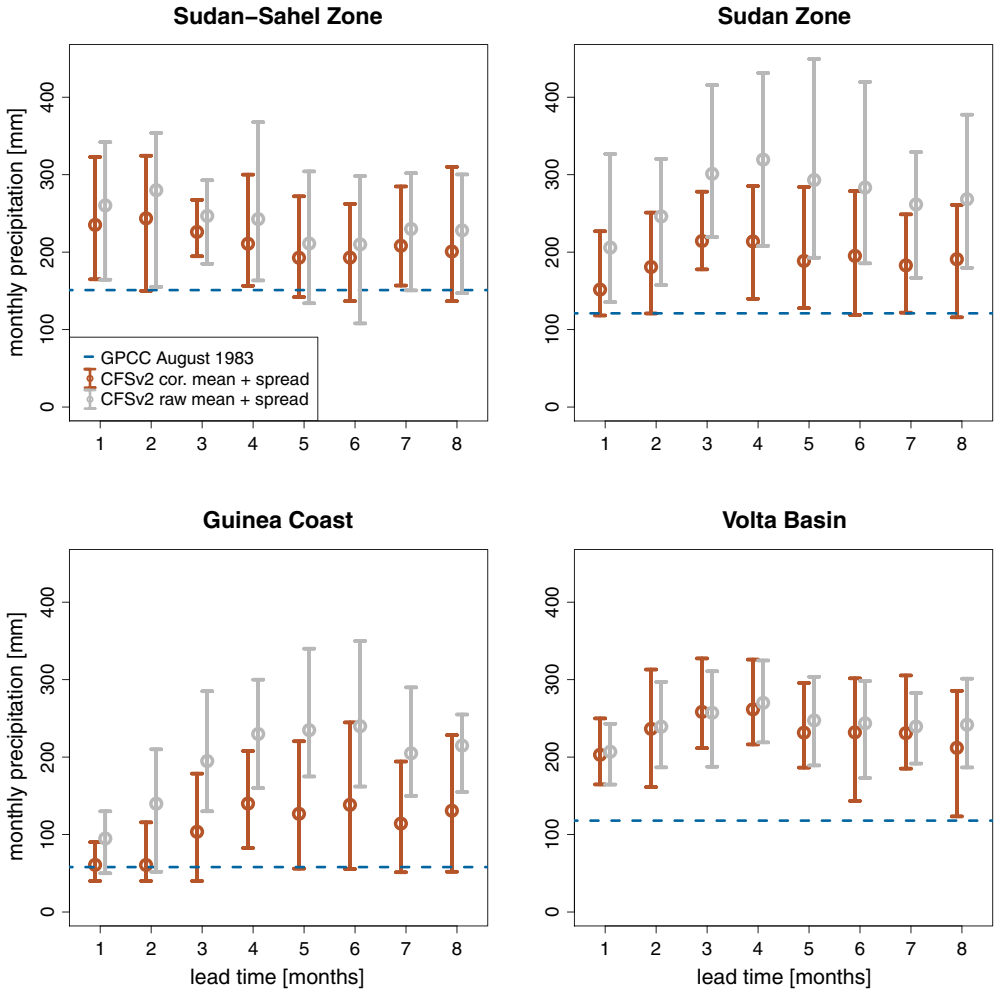

Figure 5. Corrected and raw CFSv2 reforecast ensemble spread for monthly areal precipitation for different lead times for the major drought event in August 1983. The 1 month lead time values are calculated from an ensemble initialized in July 1983, and the 8 months lead time values are calculated from an ensemble initialized in December 1982.

precipitation amount within all lead times, with the general tendency that the ensemble spread of the corrected forecast is lower and the ensemble mean of the corrected forecast is closer to the observations. The figure also illustrates that the forecast accuracy of the different CFSv2 ensembles does not steadily increase with decreasing lead time in all zones. For instance, the ensemble means with 5 and 6 months lead time in the Sudan-Sahel zone are closer to the observations than the ensemble means with lower lead times. A different picture is given for the Sudan zone, the Guinea Coast, and the Volta Basin. For these zones the means of the ensembles with 1 month lead time are closest to the observations with a tendency of a decreasing forecast accuracy for longer lead times from 1 to 4 months lead time. The ensembles with lead times of 4 and more months have likely the same inaccuracy for these zones. Furthermore, the forecast uncertainty of the ensembles with shorter lead times is not generally lower than the forecast uncertainty of ensembles with longer lead times. Only at the Guinea Coast the ensemble with 1 month lead times has a much smaller uncertainty than the ensembles with longer lead times. Figures 4 and 5 illustrate that the ensemble mean of the raw and corrected CFSv2 forecast is not the best indicator for a warning of precipitation deficit or excess. For drought or strong precipitation warnings it is certainly better to select a lower and higher quantile, respectively.

The corrected and raw CFSv2 reforecasts for the monthly areal precipitation amount of the three subzones of the Volta Basin and the Volta Basin itself are given for each August of the investigation period in Figure 6. The observations are sorted from the lowest to the highest precipitation amount of the investigation period. The monthly precipitation amounts of the raw CFSv2 6 months lead time reforecasts are considerably too high for almost all August months of the 28 years in the Guinean Coast and the Sudan zone. In the Sudan-Sahel zone,

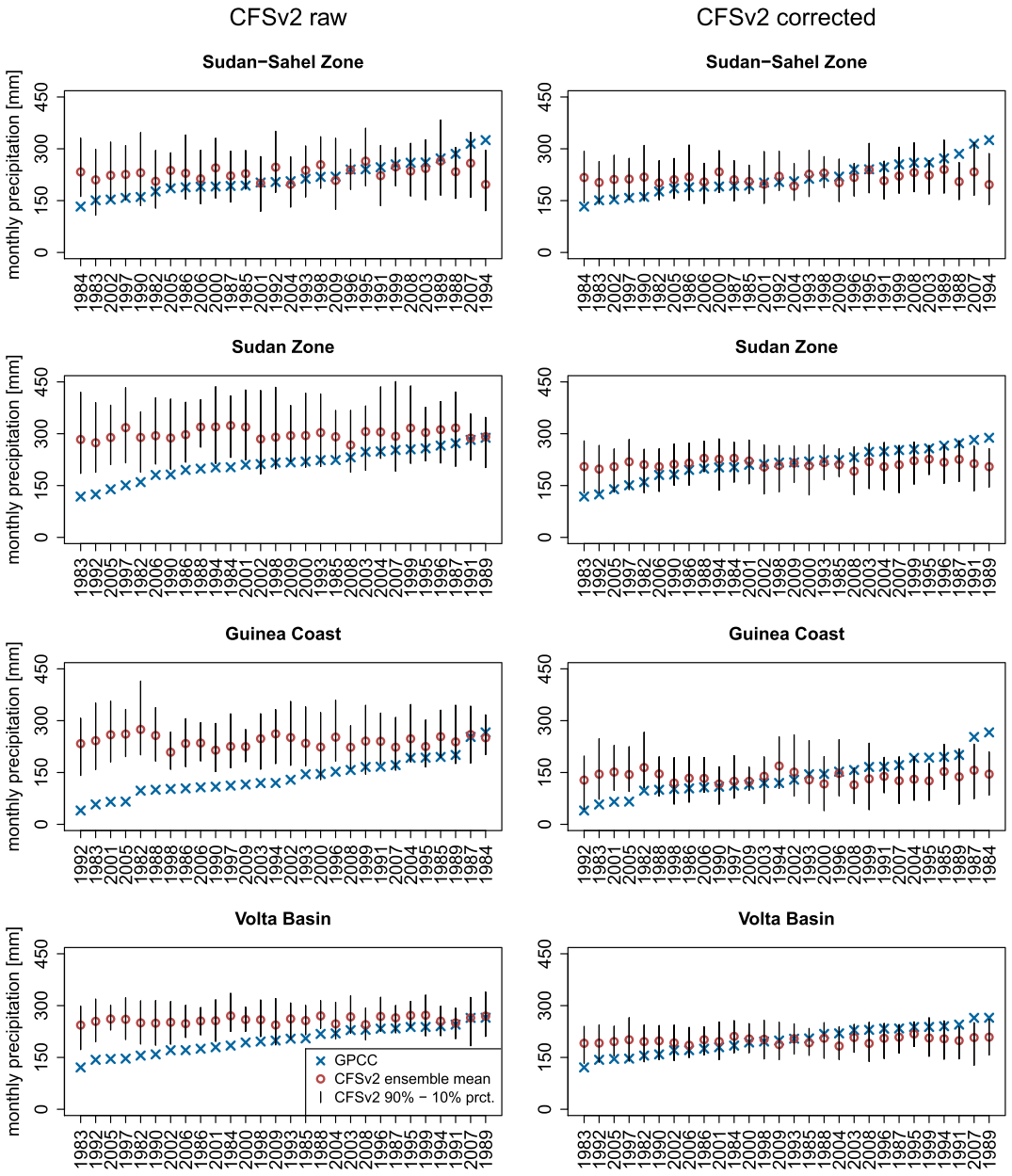

Figure 6. Predicted (6 months lead time CFSv2 reforecast ensembles) and measured (GPCC) monthly areal precipitation for the Volta Basin, August 1983–2009. Spread: 10th–90th ensemble percentile. The years are sorted from the lowest to the highest observed precipitation amount.

the forecasts are generally in the range of the observations, but the ensemble means only show very small interannual variability in all subregions (66 mm Guinea Coast, 56 mm Sudan zone, 68 mm Sudan-Sahel zone, and 29 mm for the entire Volta Basin) while the observed variability is much higher (226 mm, 170 mm, 192 mm, and 143 mm, same order as before). Furthermore, the ensemble means do not show a general increasing tendency with increasing observations. The monthly precipitation amounts of the corrected CFSv2 6 months lead time reforecasts, in general, are in the range of the observations for all August months of the 28 years in all of the subzones. But still, the ensemble means in all subregions only show very small interannual variability (55 mm Guinea Coast, 37 mm Sudan zone, 48 mm Sudan-Sahel zone, and 35 mm for the entire Volta Basin). Similar to the raw CFSv2 data, an increasing tendency of the ensemble mean with increasing observations is difficult to identify.

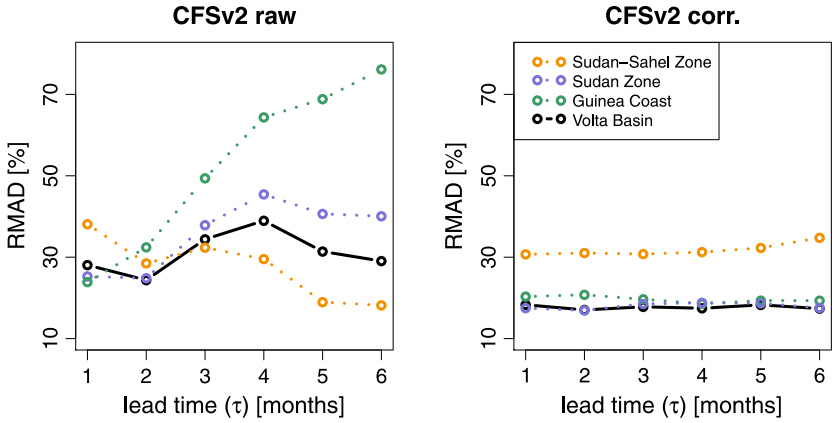

Figure 7. RMAD for the raw and corrected CFSv2 reforecast ensemble means with various lead times for the target month August. RMAD is the mean absolute distance between the ensemble mean and the corresponding GPCC observation, divided by the mean (1971–2010) GPCC observation in percent; see equation (2). The RMAD ranges between 0% and positive infinite where a low value indicates a high accuracy. With a RMAD of zero a forecast would be identical to the GPCC observations.

The ensemble spreads are very wide in all cases of the raw CFSv2 reforecasts, in some years even as wide as the GPCC variability. This indicates a high uncertainty of the ensemble forecasts, limiting their suitability for drought warnings. Despite the wide ensemble spreads, the observations are out of the range of the forecast ensembles for all subzones in most of the drier years. Since the bias correction smallered the ensemble spread, the observations now are captured by the forecast in most of the years. But still, the driest and wettest years are not within the ensemble spread in all four subregions.

The forecast accuracy of the uncorrected and corrected CFSv2 precipitation forecasts for six different lead times is illustrated in Figure 7. The statistical correction can clearly improve the forecast accuracy for the Guinean Coast, the Sudan zone, and the Volta Basin for all lead times but not for the Sudan-Sahel zone. The forecast accuracy of the uncorrected reforecasts differs considerably for the subregions. For the Guinea Coast, the RMAD decreases by decreasing lead time, while for the Sudan zone and the Sudan-Sahel zone this characteristic is not shown. The RMAD values for all three subregions are at a similar value of around 30% for the 1 and 2 months lead time ensembles. However, at longer lead times (5 to 6 months) the deviations between forecasts and observations for the Guinea Coast are considerably higher than for the other subzones, reaching up to 80% of the GPCC climatological mean. In contrast to this, the RMAD values of the corrected CFSv2 reforecasts are very similar for all lead times. The accuracies of the forecasts for the two southern zones as well as for the entire Volta Basin are around 20% of the climatological mean. In the case of the Sudan-Sahel zone the RMAD is slightly higher but does not exceed 35%.

The relative measures for describing the forecast uncertainty of the uncorrected and corrected CFSv2 reforecasts for the West African study area are indicated in Figure 8 for six different lead times. The statistical correction can clearly reduce the forecast uncertainty for all geographical regions and for all lead times. The RIDR values of the uncorrected CFSv2 reforecasts do not generally decrease or increase by decreasing lead time. Furthermore, for every lead time and all zones the RIDR is larger than 1 (red line), indicating that the ensemble spread of the CFSv2 forecasts is higher than the observed variability based on the GPCC information. This high forecast uncertainty (reaching up to almost 200% of the observed natural variability at the Sudan-Sahel zone) is a very adverse characteristic of the CFSv2 reforecasts. The RIDR values of the corrected CFSv2 reforecasts are all close to 1, meaning that the corrected CFSv2 reforecasts still are characterized by an uncertainty that is very similar to the observed variability, in particular for longer lead times. However, for both shortest lead times RIDR slightly decreases below 1 illustrating that there is a tendency that the corrected ensemble spread is slightly smaller in comparison to the observed variability.

Figure 9 shows the accuracy of the corrected and the uncorrected CFSv2 precipitation forecast for different lead times in comparison to the accuracy of the climatological forecast based on the ranked probability score. This information can also be used to determine the skill of the CFSv2 precipitation forecasts. A positive skill is indicated when the RPS of the CFSv2 precipitation forecast is below the RPS of the climatological forecast. Figure 9 indicates that the applied statistical correction method can clearly improve the CFSv2 precipitation

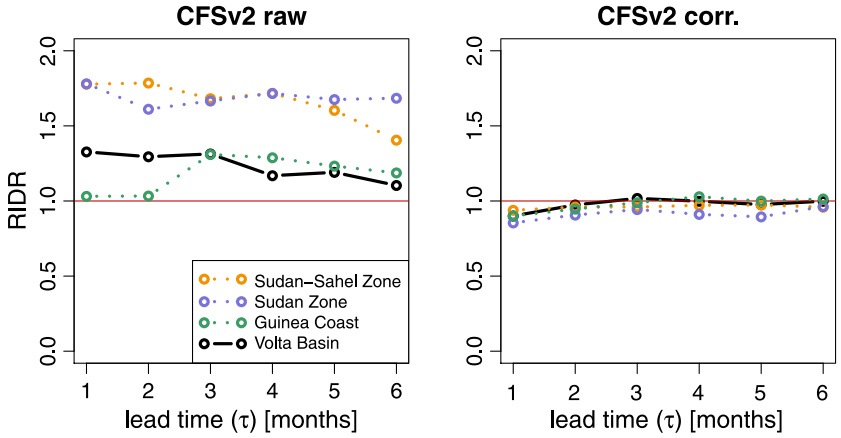

Figure 8. RIDR (see equation (1)) for various lead times out of 28 years (1982–2009) raw and corrected CFSv2 reforecasts for the target month August. RIDR is the interdecile range of the ensemble forecast (IDR_y) for August, divided by the interdecile range of the GPCC observations for all Augusts. RIDR is an expression of uncertainty where values smaller than 1 (red line) indicate forecasts with uncertainties that are smaller than the natural variability.

forecasts for the different lead times and for all geographical regions removing the strong negative skill of the uncorrected CFSv2 precipitation forecasts. However, the corrected CFSv2 precipitation forecasts are only slightly better in comparison to the climatological forecasts. For certain lead times and geographical regions, the corrected CFSv2 forecasts show still a negative skill. The skill of the corrected CFSv2 precipitation forecast when this information is used for a warning is illustrated for the different geographical regions and lead times in the ROC diagrams of Figures 10 and 11. The diagonal of the ROC diagram shows the zero skill line ($H = F$). The larger the area between a curve and the diagonal of a ROC diagram, the higher the skill of the corrected CFSv2 precipitation forecast. In addition, the individual PSS skill scores of the corrected CFSv2 forecasts are

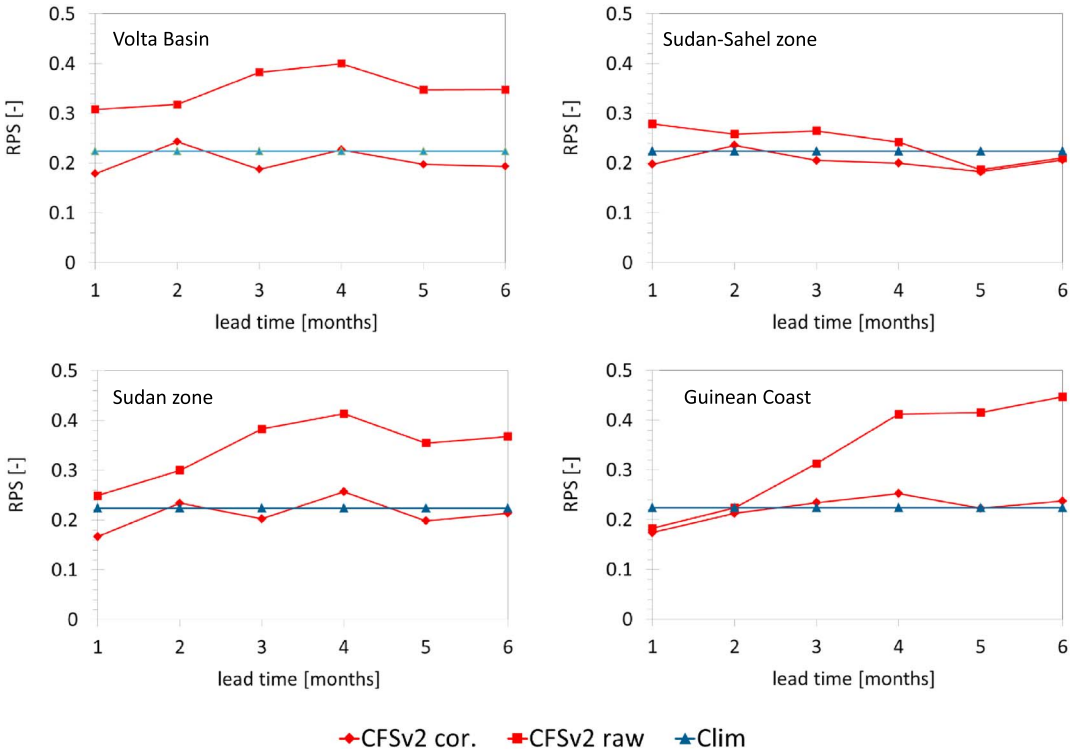

Figure 9. The performance of the corrected and raw CFSv2 precipitation forecasts for different lead times and the different study regions using the ranked probability score (RPS) in comparison to the climatological forecasts for the target month August 1982–2009.

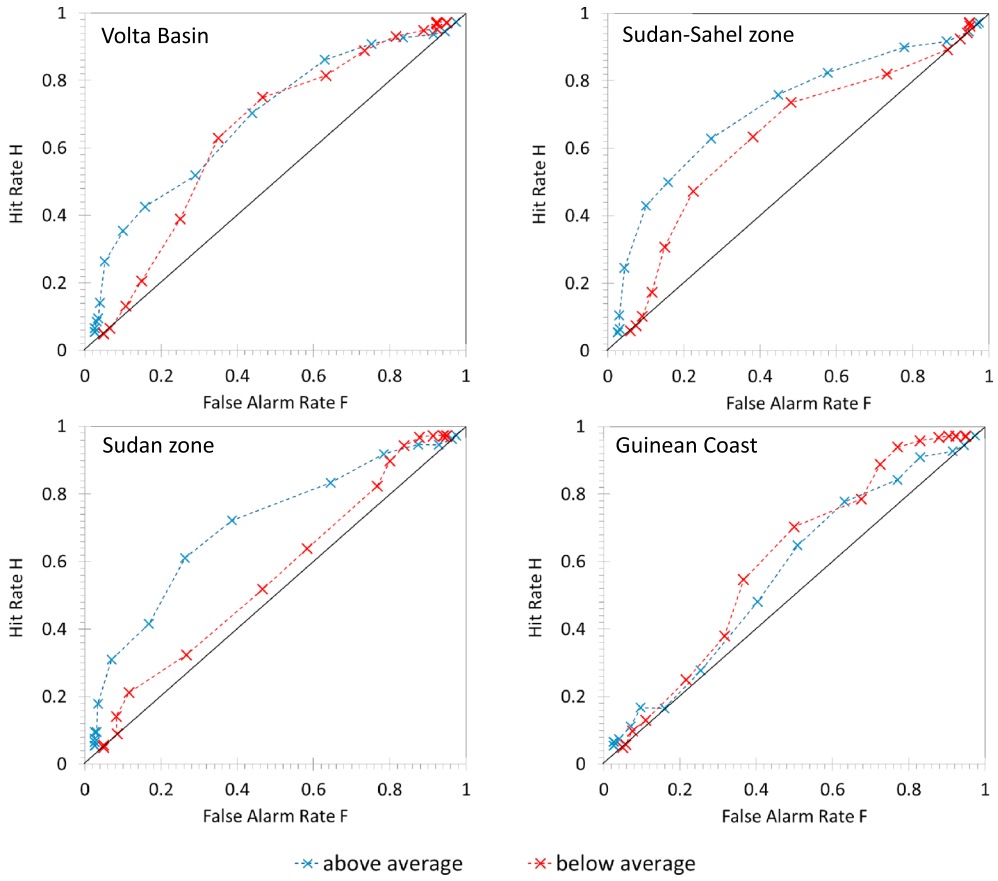

Figure 10. The relative operating characteristics (ROC) for the individual zones as an average over six lead times for above average (precipitation excess) and below average (precipitation deficit) events, corrected CFSv2 precipitation forecasts, August months from 1982 to 2009. The diagonal in the ROC diagram indicates the no skill line ($H = F$).

listed in Table 1 for all geographical regions, lead times, and events based on the assumption that the optimal probability threshold is used for decision-making. The ROC diagrams and PSS indicate a low to moderate skill of the corrected CFSv2 precipitation forecasts when this information is used for a warning for all geographical regions, lead times, and both event types. However, the performance of the forecasting system depends on the geographical region and the lead time and the event considered. In general, the CFSv2 precipitation forecasts are more skillful for the Sudan-Sahel zone (mean PSS = 0.365) in comparison to the Sudan zone (mean PSS = 0.295) and the Guinean Coast (mean PSS = 0.262). The CFSv2 precipitation forecasts are slightly better for precipitation excess (mean PSS = 0.345) than for precipitation deficits (mean PSS = 0.270). The CFSv2 precipitation forecasts are positive for all lead times with the highest skill for the first month (mean PSS = 0.469) and moderate skills for the fifth month (mean PSS = 0.318) and sixth month (mean PSS = 0.284). However, the skill of the CFS precipitation forecast is not monotonically decreasing with increasing lead time as indicated in the ROC diagrams. The lowest performance is given for the fourth month (mean PSS = 0.173). Since the PSS is identical to the maximum economic value, the maximum economic value of the corrected CFS forecast system ranges between 0.029 and 0.626 with a total mean of 0.307 indicating that the corrected CFS precipitation forecasts have the potential to provide valuable information regarding the warning of precipitation anomalies in August in this region.

4.2. CFSv2-WRF Results for Monthly Precipitation and Intraseasonal Rainfall Characteristics

The CFSv2-WRF forecasts of the monthly precipitation amount for the three subregions and the entire Volta Basin for the rainy season 2013 in comparison to the raw and corrected CFSv2 and the GPCC climatology forecasts are illustrated in Figure 12. The climatology forecast is based on 40 years (1971–2010) of the GPCC data period. The forecasts are compared the GPCC first guess precipitation data. The comparison of the

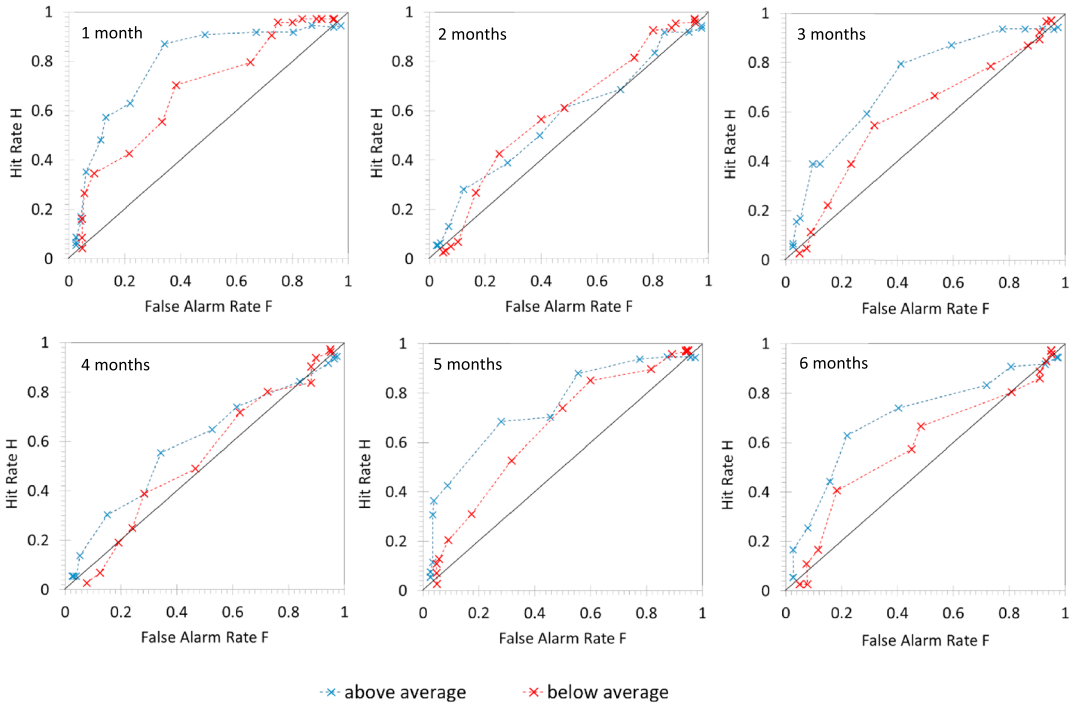

Figure 11. The relative operating characteristics (ROC) for the individual lead times as an areal weighted average of the three agroecological zones of the Volta Basin for above average (precipitation excess) and below average (precipitation deficit) events, corrected CFSv2 precipitation forecasts, August months from 1982 to 2009. The diagonal in the ROC diagram indicates the no skill line ($H = F$).

corrected CFSv2 and CFSv2-WRF ensembles with the observational data shows that in the Sudan-Sahel zone the CFSv2 ensemble mean is close to the observations. The WRF ensemble still covers the observational data for the first 3 months, while from June to August the entire ensemble underestimates the observed precipitation amounts. In the Sudan zone the observations are only located within the corrected CFSv2 ensemble spread from March to June. In contrast to this, the CFSv2-WRF ensemble covers the GPCC first guess observations for most of the months, especially during the summer. The GPCC climatology forecast shows that the rainy season 2013 was not very unusual in the Sudan-Sahel zone and the Sudan zone and thus could very well be forecasted by the climatologic mean, whereas June 2013 was unusually dry at the Guinea Coast, and thus, the observations are outside the ensemble spread of the climatology forecast ensemble. In this zone, only the CFSv2-WRF ensemble predicted the very dry conditions in June, while CFSv2 and CFSv2-WRF could not predict the conditions in July and August. There is a major mismatch between the forecasted and observed precipitation amounts in the time between the two rainy seasons (July and August) at the Guinean Coast, in particular for the CFSv2-WRF ensemble.

Table 1. The Peirce Skill Score of the Corrected CFSv2 Precipitation Forecasts Determined for Each Geographical Region of the Volta Basin, Event Category (Below = Precipitation Excess, Above = Precipitation Deficit), and for Six Lead Times (Months)[a]

Region	Event Category	1	2	3	4	5	6
Sudan-Sahel	Below	0.311	0.156	0.256	0.289	0.344	0.400
Sudan-Sahel	Above	0.521	0.175	0.392	0.456	0.567	0.509
Guinean	Below	0.499	0.522	0.411	0.144	0.233	0.056
Guinean	Above	0.415	0.298	0.099	0.029	0.175	0.257
Sudan	Below	0.444	0.133	0.222	0.067	0.238	0.133
Sudan	Above	0.626	0.351	0.573	0.056	0.351	0.351

[a]The Peirce skills score is a measure for the skill of binary forecasting system and is identical to maximum economic value of a warning system. August months of 1982 to 2009.

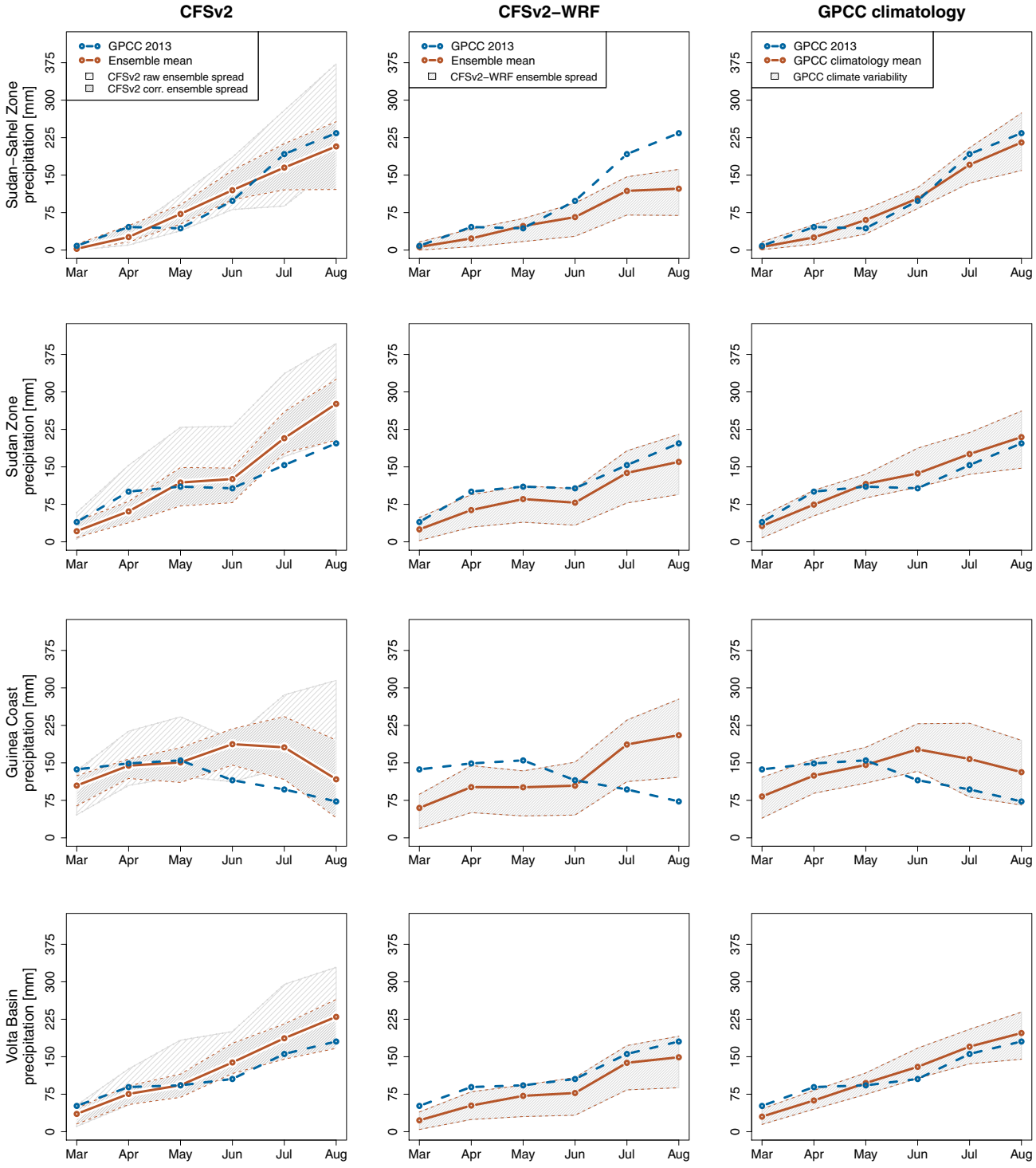

Figure 12. Seasonal raw and corrected CFSv2, CFSv2-WRF, and GPCC climatology forecasts for monthly areal precipitation at the three agroecological zones of the Volta Basin for the rainy season 2013 in comparison to GPCC first guess. CFSv2 and CFSv2-WRF ensembles are built out of the 22 CFSv2 simulation runs initialized in February 2013; the GPCC climatology forecast is based on the observed variability of 40 years of GPCC observations (1971–2010). The shaded areas cover the ensemble spread (10th–90th percentiles) for the forecast.

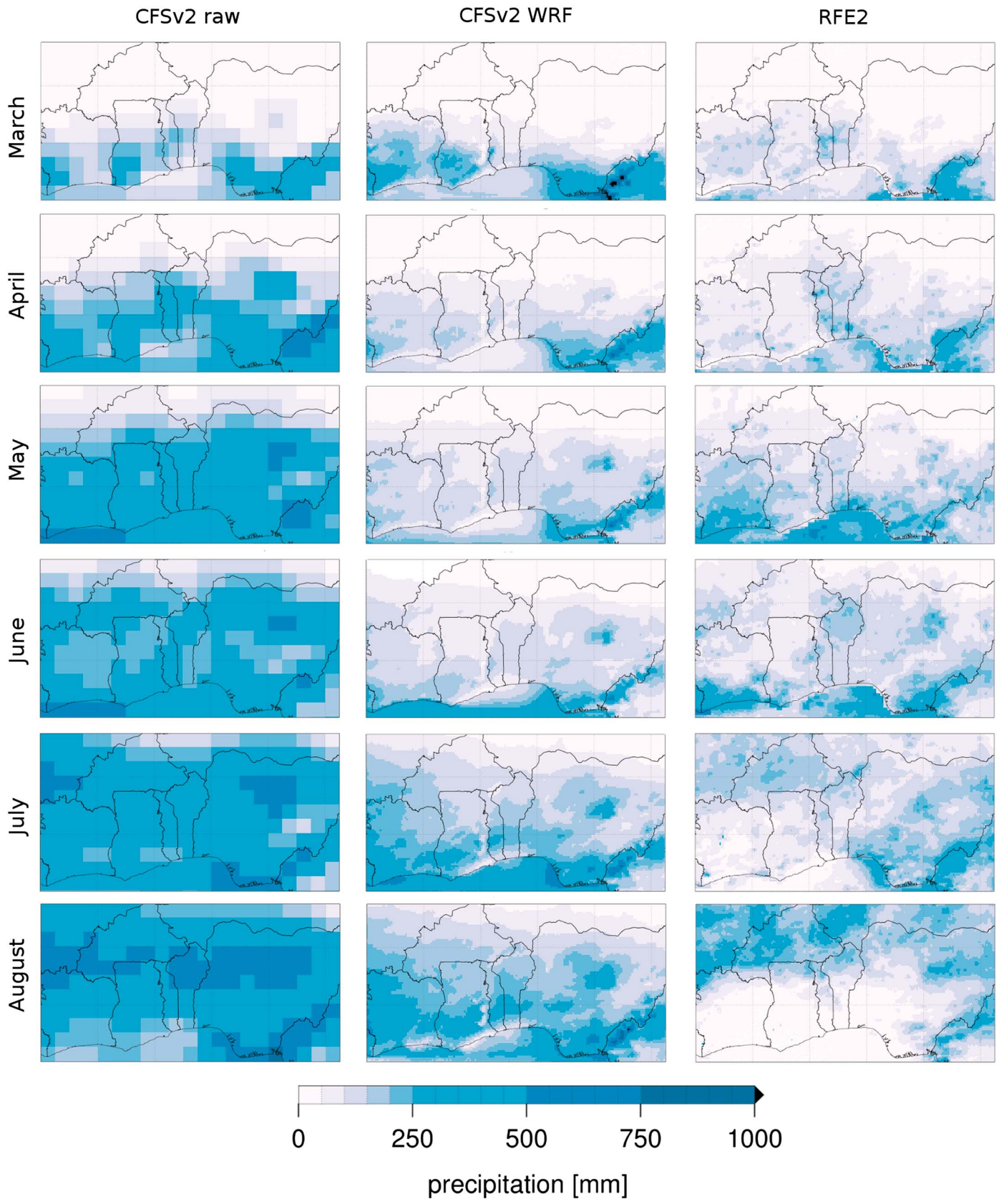

Figure 13. Monthly precipitation amount (mm) of the CFSv2 and CFSv2-WRF ensemble mean (each from 22 members of the ensemble initialized in February) compared to the RFE2 measurements for the rainy season 2013.

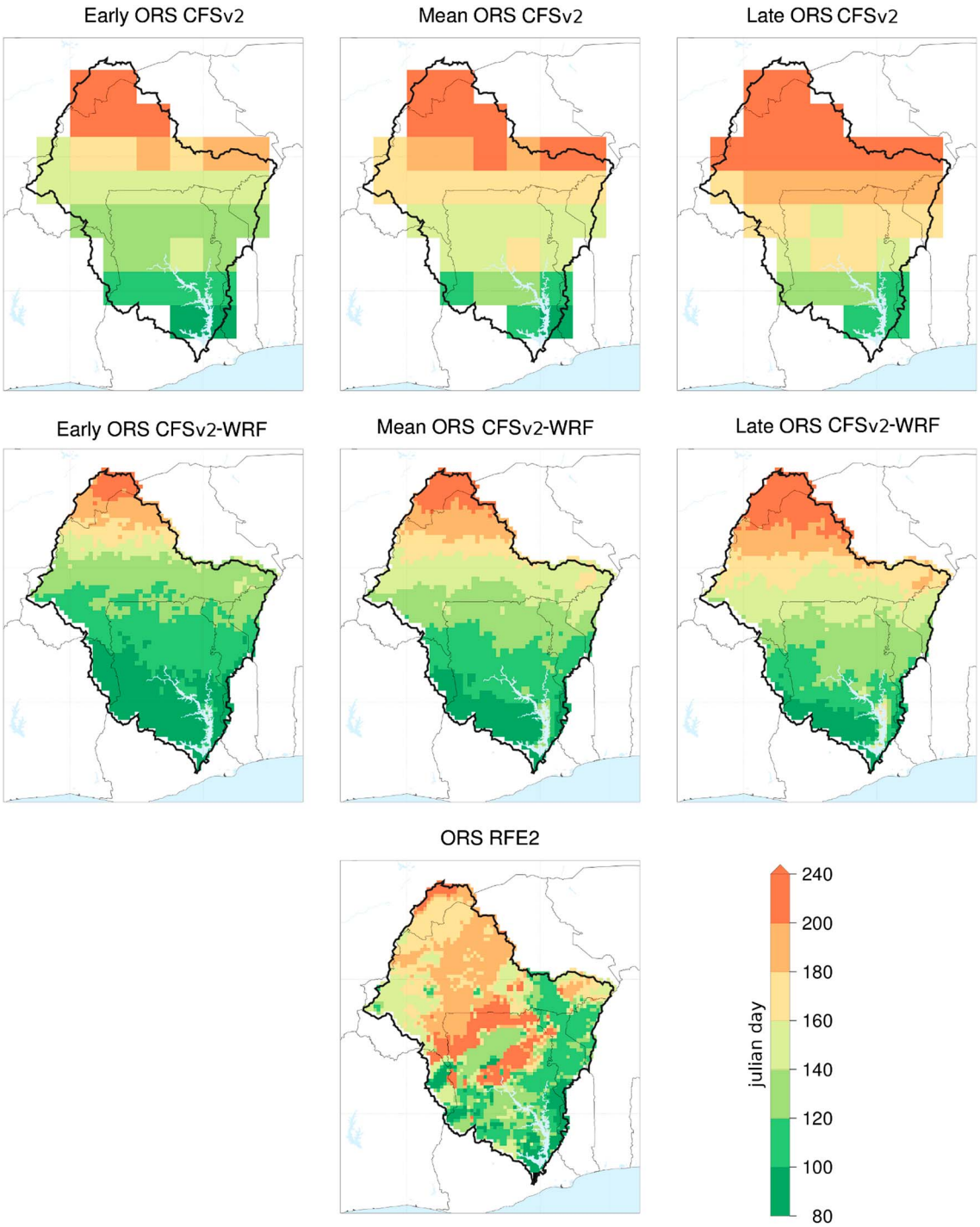

Figure 14. The predicted date of the onset of the rainy season (ORS in Julian days), of the CFSv2 raw ensemble, CFSv2-WRF ensemble in comparison to the ORS dates calculated from RFE2 observations. The *early ORS* is the 25th percentile of the ORS dates from the 22 ensemble members, and *late ORS* is based on the corresponding 75th percentile. It is noted that the ORS distribution calculated from the RFE2 data set is quite unusual in northern an central Ghana. The very late onset dates in 2013 result from very unusually dry conditions during June in this region.

The spatial distribution of the predicted monthly precipitation amount for the entire forecast period is illustrated in Figure 13 using the ensemble mean. The predicted information is compared to the observed monthly precipitation amount taken from the RFE2 data set. Due to the finer resolution, the downscaled monthly precipitation shows considerably finer detailed information. The raw CFSv2 ensemble shows only weak zonal differentiations and too high rainfall amounts in many parts of the simulation domain. The CFSv2-WRF ensemble's rainfall patterns against this show a clear north-south gradient and specific local rainfall characteristics like the anomalous dry conditions around the coastal region of Ghana, Togo, and Benin (*Dahomey Gap*). But the characteristic midsummer dry period through July and August at the Guinean Coast is not represented in both ensemble forecasts. During the months July and August, the rain belt of the CFSv2-WRF ensemble does not or too slowly penetrate northward. This results in too high precipitation amounts in the southern and too low precipitation amounts in the northern regions of the domain, compared to the RFE2 map.

The predicted onset of the rainy season (ORS) dates for the raw CFSv2 and the CFSv2-WRF data sets is illustrated in Figure 14 for the Volta Basin and compared to the observed ORS dates calculated from the RFE2 observations. The figure shows the mean date of the ORS and early and late dates of the ORS to illustrate the uncertainty of the forecast for this specific variable. The early and late dates of the ORS are based on the 25th and 75th percentiles of the calculated ORS dates of the forecast ensemble. The observed ORS dates (ORS RFE2) show a clear north-south gradient that is disturbed by a very high spatial variability. In large parts of northern Ghana the ORS was very late in 2013 (between 19 July and 28 August). In contrast, both modeled ORS dates are comparatively smooth, resulting from the averaging of 22 ensemble members. The maps of the single ensemble members (not shown) produce a similar variability as the RFE2 map.

The ORS dates calculated from the CFSv2 ensemble are too late for large parts of the northern Volta Basin. Against this, the CFSv2-WRF-derived ORS dates are closer to the observations in amplitude and spatial differentiation in this region. In the very southern part, the CFSv2 ORS dates are near to the observed dates, referring to their general amplitude while the CFSv2-WRF ORS dates are mainly too early. To be highlighted here is the following: the unusually late onset dates in central Ghana (resulting from the dry June) can be seen in the CFSv2 ORS dates (indicated by the orange pixel) even though the absolute date is too early. The CFSv2-WRF ensemble does not show this pattern. The ORS date spread (range from the "early ORS" to the "late ORS") of the CFSv2 maps is very large all over the Volta Basin, even up to 60 days for parts of Burkina Faso. Against this, the ORS date spread of the CFSv2-WRF ensemble has (except for the very eastern part of the Volta Basin) a maximum of 20 days and thus has a lower uncertainty.

5. Summary and Discussion

In this study we investigated the forecast performance of the monthly precipitation forecast of NOAA's CFSv2 by using the raw and corrected precipitation reforecast with a special focus on three agroecological zones of the Volta Basin for all August months of the period ranging from 1982 to 2009. The precipitation reforecast of CFSv2 is corrected by using a quantile-quantile transformation for eliminating systematic differences between reforecasts and observations. The corrected and raw precipitation forecasts are compared to a climatological forecast and GPCC observations using the ranked probability score, the ROC diagram, and the Peirce skill score as a measure for the maximum economic value. Since GSEPS precipitation forecasts are often used in distributed modeling approaches, e.g., in hydrology or agriculture, an evaluation of the forecast accuracy and uncertainty is also performed in the physical space using a standard measure for determining the forecast accuracy and a novel relative measure that addresses the forecast uncertainty of an ensemble forecast in comparison to the observational uncertainty.

In a first step, we analyzed the raw and corrected CFSv2 monthly precipitation reforecasts for one single drought event 1983. In all three zones the precipitation during the unusual dry conditions of the central months of the rainy season 1983 has been overestimated by the raw and the corrected reforecast ensemble, but the statistical correction clearly reduces the ensemble spread and improves the accuracy for various lead times. Even though the ensemble spread was very large, the observations in some cases were not even covered by the lowest ensemble member. The analysis of the corrected and raw CFSv2 precipitation forecasts for the August months of the entire data period from 1982 to 2009 shows that the raw CFSv2 strongly overestimates precipitation amounts for dry August months and for all regions. This overestimation can be reduced when the statistical correction is applied to the CFSv2 precipitation forecasts. However, both raw and corrected forecasts show only very small interannual variability all over the Volta Basin from 1982 to 2009.

The introduction of the novel relative measure highlighted a CFSv2 ensemble spread of the raw precipitation forecasts which is clearly larger than the observed variability. This strong overestimation in terms of variability can be reduced by using the selected quantile-quantile transformation. The corrected CFSv2 precipitation forecast is for various lead times and agroecological zones even slightly better in comparison to a climatological forecast, as the ranked probability score indicates a positive skill. This outcome confirms the general findings of the study of *Zuo et al.* [2013] which was done on a much broader scale for our study region. In addition to the study of *Zuo et al.* [2013], we also assessed the skill and forecast value (the economic value) of using the CFSv2 precipitation forecast for an early warning of upcoming precipitation deficits and excess in this region. We illustrated a low to moderate skill up to six 6 months in advance for all three geographical regions and for both event types when the corrected CFSv2 forecast is used for a warning. The maximum economic value of this warning system ranges between 0.029 and 0.626 with an average of 0.307 indicating the potential of providing valuable seasonal precipitation forecasts for this region based on corrected CFSv2 precipitation forecast. In order to better understand the reasons for CFSv2's general overestimation of rainfall in West Africa, in-depth and process-based analyses of the CFSv2 forecasts are necessary to figure out which large-scale processes of the West African monsoon system can adequately be forecasted and which cannot. Since the reasons for the Sahel drought 1983 were extraordinary SST anomalies in the Indian and tropical eastern Atlantic Ocean [*Bader and Latif*, 2011; *Nicholson*, 2009], analyses regarding a proper reproduction of these SST patterns by CFSv2 are of high importance for future studies. In addition, future contributions should consider additional drought events to obtain a more general view of the usability of the CFSv2 product for drought prediction.

In a second step, we conducted a dynamical ensemble downscaling approach using WRF, driven by the operational seasonal CFSv2 forecasts. The downscaling was performed for the rainy season 2013 using a subset of the CFSv2 9 months forecast initialized in February. While some studies already investigated dynamical and statistical downscaling approaches for the CFSv2 reforecasts in other regions of the world [*Huang and Chan*, 2013; *Yuan et al.*, 2013b], the only study dealing with a downscaling technique for West Africa based on CFSv2 seems to be the study presented by *Yuan et al.* [2013a] using a Bayesian merging method. The downscaling of *Yuan et al.* [2013a] did allow only a slight improvement of the raw CFSv2 drought forecast for lead times longer than 1 month. In a study by *Castro* [2012] for North America, the WRF downscaling of CFS1 Reforecasts led to improvements in many aspects of the seasonal forecasts.

In this study CFSv2-WRF was compared to the raw and statistically corrected CFSv2 precipitation forecasts, a climatological forecast, and in comparison to observational data sets. The target variables of this study were monthly rainfall information (aggregated from daily data) and the agriculturally relevant date of the onset of the rainy season (ORS). This intraseasonal precipitation feature jointly accounts for daily rainfall amounts, the number of wet days, and dry spell criteria. Predicted ORS dates are highly desired by local agriculture in West Africa [*Roncoli et al.*, 2002] and many other parts of the tropics. The seasonal predictability of ORS dates for other regions of the world has formerly been analyzed using sets of GCM reforecasts with a combination of various statistical techniques by *Moron et al.* [2006] for Senegal and *Robertson et al.* [2009] for Indonesia. *Vellinga et al.* [2013] analyzed the predictability of the monsoon onset using UK's seasonal forecasting system (GloSea4) and found modest results.

Compared to the CFSv2 raw data, the downscaling showed marginal improvements of total rainfall amounts for the Volta Basin. The forecast uncertainty, expressed by the ensemble spread, was clearly reduced in comparison to the raw CFSv2 forecast but not in comparison to the corrected CFSv2 forecast. A severe CFSv2-WRF deficit was found for the downscaling approach regarding the seasonality of monthly precipitation patterns during July and August due to a reduced movement of the monsoonal rain belt. Although the downscaling can reduce an overestimation of the CFSv2 raw precipitation forecasts from March to June, the midsummer dry period in July and August at the Guinean Coast was not reproduced. In case of the ORS dates, the CFSv2-WRF ensemble better represents the spatial distribution of the observed ORS dates and the dates are in a more realistic range than the CFSv2 ORS dates, especially in the northern part of the study area. Since the monthly precipitation patterns are used by distributed modeling approaches in hydrology, agriculture, and further fields, future contributions should focus on an in-depth evaluation of the spatial precipitation patterns forecasts by GSEPS using corresponding measures for field verification. For future studies it will also be of importance to give physical insights into the representation of important atmospheric features like the Tropical Easterly Jet and the African Easterly Jet in both the raw and WRF-downscaled CFSv2 forecasts.

This study presented a first analysis whether a statistical correction and dynamical downscaling of a GSEPS could be a valuable addition to the current operational PRESAO practice in West Africa. The selected approaches can be adequate techniques to cope with the limitations of the seasonal PRESAO forecasts, especially concerning the temporal and spatial resolution, the lead time, and the possibility to derive intraseasonal precipitation characteristics. The selection of the quantile-quantile transformation for a correction of the raw CFS precipitation forecast seems to be a promising technique indicated by a low positive skill. In comparison to the dynamical downscaling approach, this technique is not computational demanding and can be also easily implemented on personal computer at the national weather services. The corrected CFSv2 reforecasts are in observation ranges but have still deficits at the very dry and very wet years. The outcomes of the dynamical downscaling experiment offered first promising results but also showed a clear deficiency. In order to further improve the current downscaling approach, further simulation experiments are necessary to improve the modeled movement of the ITCZ within CFSv2-WRF. According to *Nicholson* [2009], the main influencing factors for the positioning of the monsoonal rain belt are the positions of the African Easterly Jet and the Tropical Easterly Jet. *Klein et al.* [2015] showed that changing a parameterization scheme can have a strong influence on the positions of both jets so that changing the current parameterization schemes might improve the movement of the rain belt. In addition, systematic investigations for multiple years are necessary to generally assess the added value of this technique. To perform such experiments, it is inevitable that the operational CFSv2 forecasts are stored in full vertical resolution for future years and full reforecasts are available for the entire period 1982–2009 or for selected years. For the application of a time-consuming and computational demanding dynamical downscaling in the framework of African meteorological services, it would be also desirable to develop a technique to reduce the ensemble size while conserving the specific characteristics of an ensemble forecast.

Acknowledgments

This study was embedded within the Core Research Program of the West African Science Service Center on Climate Change and Adapted Land Use (www.WASCAL.org), funded by the German Federal Ministry of Education and Research (BMBF). A key activity of the climate research and service group of WASCAL is to strengthen the National Met Services in West Africa, e.g., by refining the current meteorological observation networks and their techniques used in weather forecasting. We also want to thank Andre Kamga from ACMAD for giving us the possibility to present and to share our ideas in front of the PRESAO community in May 2012 during the workshop in Ouagadougou. Many thanks also to Moussa Waongo for the fruitful discussions regarding the common practices of operational seasonal forecasts in West Africa and their limitations. Gauge data for Tamale and Ouagadougou have been kindly provided by the Ghana Meteorological Agency and Burkina Faso's General Directorate of Meteorology, respectively. Thanks to Christof Lorenz (KIT) and Thomas Rummler (University of Augsburg) for technical assistance and for providing postprocessing tools. E-mail contact for the used data sets: patrick.laux@kit.edu.

References

Bader, J., and M. Latif (2011), The 1983 drought in the West Sahel: A case study, *Clim. Dyn.*, *46*, 463–472.

Bardossy, A., and G. Pegram (2011), Downscaling precipitation using regional climate models and circulation patterns toward hydrology, *Water Resour. Res.*, *47*, W04505, doi:10.1029/2010WR009689.

Barry, B., E. Obuobie, M. Andreini, W. Andah, and M. Pluquet (2005), The Volta River Basin: Comparative study of river basin development and management, *Draft Rep.*, Compr. Assess. Water Manage. Agric. and Int. Water Manage. Inst.Colombo, Sri Lanka.

Bliefernicht, J. (2011), Probability forecasts of daily areal precipitation for small river basins, PhD thesis, vol. 194, 185 pp., Mitteilungen des Instituts für Wasserbau, Univ. Stuttgart, Germany.

Bliefernicht, J., et al. (2013), Field and simulation experiments for investigating regional land-atmosphere interactions in West Africa: Experimental set-up and first results, *Climate and Land Surface Changes in Hydrology, IAHS RedBook Ser.*, vol. 359, edited by E. Boegh et al., pp. 226–232.

Bogner, K., F. Pappenberger, and H. Cloke (2012), Technical Note: The normal quantile transformation and its application in a flood forecasting system, *Hydrol. Earth Syst. Sci.*, *16*, 1085–1094.

Castro, C. (2012), *Can a Regional Climate Model Improve the Ability to Forecast the North American Monsoon, Clim. Test Bed Joint Semin. Ser.*, pp. 1–6, US Natl. Oceanic and Atmos. Admin., NCEP, Camp Springs, Md.

Di Giuseppe, F., F. Molteni, and A. Tompkins (2013), A rainfall calibration methodology for impacts modelling based on spatial mapping, *Q. J. R. Meteorol. Soc.*, *139*, 1389–1401.

Dudhia, J. (1989), Numerical Study of convection observed during the winter monsoon experiment using a mesoscale two-dimensional model, *J. Atmos. Sci.*, *46*, 3077–3107.

Dutra, E., F. Giuseppe, F. Wetterhall, and F. Pappenberger (2013a), Seasonal forecasts of droughts in African basins using the Standardized Precipitation Index, *Hydrol. Earth Syst. Sci.*, *17*, 2359–2373.

Dutra, E., L. Magnusson, F. Wetterhall, H. Cloke, G. Balsamo, S. Boussetta, and F. Pappenberger (2013b), The 2010–2011 drought in the Horn of Africa in ECMWF reanalysis and seasonal forecast products, *Int. J. Climatol.*, *33*, 1720–1729, doi:10.1002/joc.3545.

ECMWF (2014), ECMWF seasonal forecast system 4. [Available at http://www.ecmwf.int/products/changes/system4/#description.]

Epstein, E. (1969), A scoring system for probability forecasts of ranked categories, *J. Appl. Meteorol.*, *8*(6), 985–987.

Fontaine, B., and S. Janicot (1996), Sea surface temperature fields associated with West African rainfall anomaly types, *J. Clim.*, *9*, 2935–2940.

Hansen, J., S. Mason, L. Sun, and A. Tall (2011), Review of seasonal climate forecasting for agriculture in sub-Saharan Africa, *Exp. Agric.*, *47*, 205–240.

Hogan, R., and I. Mason (2012), Deterministic forecasts of binary events, in *Forecast Verification: A Practitioner's Guide in Atmospheric Science*, edited by I. T. Jolliffe and D. B. Stephenson, pp. 31–59, John Wiley, Chichester, U. K.

Hong, S., J. Dudhia, and S. Chen (2004), A revised approach to ice microphysical processes for the bulk parameterization of clouds and precipitation, *Mon. Weather Rev.*, *132*, 103–120.

Hong, S., Y. Noh, and J. Dudhia (2006), A new vertical diffusion package with an explicit treatment of entrainment processes, *Mon. Weather Rev.*, *134*, 2318–2341.

Hu, Z., A. Kumar, B. Huang, W. Wang, J. Zhu, and C. Wen (2012), Prediction skill of monthly SST in the North Atlantic Ocean in NCEP Climate Forecast System version 2, *Clim. Dyn.*, *40*, 2745–2759.

Huang, W., and J. Chan (2013), Dynamical downscaling forecasts of Western North Pacific tropical cyclone genesis and landfall, *Clim. Dyn.*, *42*, 2227–2237, doi:10.1007/s00382-013-1747-3.

Janjic, Z. (1994), The step-mountain Eta coordinate model: Further developments of the convection, viscous sublayer, and turbulence closure schemes, *Mon. Weather Rev.*, *122*, 927–945.

Jenkins, G. (1997), The 1988 and 1990 summer season simulations for West Africa using a regional climate model, *J. Clim.*, *10*, 1255–1272.

Jolliffe, I., and D. Stephenson (Eds.) (2012), *Forecast Verification: A Practitioner's Guide in Atmospheric Science*, John Wiley, Chichester, U. K.

Jung, G., and H. Kunstmann (2007), High-resolution regional climate modelling for the Volta Basin of West Africa, *J. Geophys. Res.*, *112*, D23108, doi:10.1029/2006JD007951.

Klein, C., D. Heinzeller, J. Bliefernicht, and H. Kunstmann (2015), Variability of West African monsoon patterns generated by a WRF multi-physics ensemble, *Clim. Dyn.*, 1–23, doi:10.1007/s00382-015-2505-5.

Krzysztofowicz, R. (1997), Transformation and normalization of variates with specified distributions, *J. Hydrol.*, *197*, 286–292.

Kunstmann, H., and G. Jung (2007), Influence of soil-moisture and land use change on precipitation in the Volta Basin of West Africa, *Int. J. River Basin Manage.*, *5*, 9–16.

Laux, P., H. Kunstmann, and A. Bardossy (2008), Predicting the regional onset of the rainy season in West Africa, *Int. J. Climatol.*, *28*, 329–342.

Laux, P., S. Wagner, A. Wagner, J. Jacobeit, A. Bardossy, and H. Kunstmann (2009), Modelling daily precipitation features in the Volta Basin of West Africa, *Int. J. Climatol.*, *29*, 937–954.

Laux, P., G. Jaeckel, R. Tingem, and H. Kunstmann (2010), Impact of climate change on agricultural productivity under rainfed conditions in Cameroon—A method to improve attainable crop yields by planting date adaptations, *Agric. For. Meteorol.*, *150*, 1258–1271.

Lebel, T., F. Delclaux, L. Barbe, and J. Polcher (2000), From GCM scales to hydrological scales: Rainfall variability in West Africa, *Stochastic Environ. Res. Risk Assess.*, *14*, 275–295.

Liu, B., K. Costa, L. Xie, and F. Semazzi (2014), Dynamical downscaling of climate change impacts on wind energy resources in the contiguous United States by using a limited-area model with scale-selective data assimilation, *Adv. Meteorol.*, *2014*, 1–11.

Lorenz, C., and H. Kunstmann (2012), The hydrological cycle in three state-of-the-art reanalyses: Intercomparison and performance analysis, *J. Hydrometeorol.*, *13*, 1379–1420.

Mason, S., and S. Chidzambwa (2009), Position Paper: Verification of African RCOF Forecasts, Columbia Univ. Acad. Commons. [Available at http://hdl.handle.net/10022/AC:P:8908.]

Mlawer, E. J., S. J. Taubman, P. D. Brown, M. J. Iacono, and S. A. Clough (1997), Radiative transfer for inhomogeneous atmospheres: RRTM, a validated correlated-k model for the longwave, *J. Geophys. Res.*, *102*, 16663–16,682.

Moron, V., A. Robertson, and M. Ward (2006), Seasonal predictability and spatial coherence of rainfall characteristics in the tropical setting of Senegal, *Mon. Weather Rev.*, *134*, 3248–3262.

Moron, V., P. Camberlin, and A. Robertson (2013), Extracting subseasonal scenarios: An alternative method to analyze seasonal predictability of regional-scale tropical rainfall, *J. Clim.*, *26*, 2580–2600.

Mwangi, E., F. Wetterhall, E. Dutra, F. Di Giuseppe, and F. Pappenberger (2014), Forecasting droughts in Africa, *Hydrol. Earth Syst. Sci.*, *18*, 611–620.

NCEP (2013), Summary of available products from CFSv2 Real Time Forecasts. NOAA. [Available at http://cfs.ncep.noaa.gov/cfsv2/docs.html.]

Ndiaye, O., L. Goddard, and L. Ward (2009), Using regional wind fields to improve general circulation model forecasts of July–September Sahel rainfall, *Int. J. Climatol.*, *29*, 1262–1275.

Ndiaye, O., M. Ward, and W. Thaiw (2011), Predictability of seasonal Sahel rainfall using GCMs and lead-time improvements through the use of a coupled model, *J. Clim.*, *24*, 1931–1949.

Nicholson, S. (2001), Climatic and environmental change in Africa during the last two centuries, *Clim. Res.*, *17*, 123–144.

Nicholson, S. (2009), A revised picture of the structure of the "monsoon" and land ITCZ over West Africa, *Clim. Dyn.*, *32*, 1155–1171.

Nicholson, S. (2013), The West African Sahel: A review of recent studies on the rainfall regime and its interannual variability, *ISRN Meteorol.*, *2013*, 453521.

NOAA (2014), 7 days rotating archive of the CFSv2 operational seasonal forecasts. [Available at http://nomads.ncep.noaa.gov/pub/data/nccf/com/cfs/prod/cfs/.]

NOAA (2014), NCEP Climate Forecast System version 2, data access. [Available at http://nomads.ncdc.noaa.gov/data.php?name=access\#cfs-refor-data.]

NOAA CPC (2013), African rainfall estimates. [Available at http://www.cpc.ncep.noaa.gov/products/fews/rfe.shtml.]

Paeth, H., et al. (2011), Progress in regional downscaling of West African precipitation, *Atmos. Sci. Lett.*, *12*, 75–82.

Richardson, D. (2003), Economic value and skill, in *Forecast Verification: A Practitioner's Guide in Atmospheric Science*, edited by I. T. Jolliffe and D. B. Stephenson, pp. 167–184, John Wiley, Chichester, U. K.

Robertson, A., V. Moron, and Y. Swarinoto (2009), Seasonal predictability of daily rainfall statistics over Indramayu district, Indonesia, *Int. J. Climatol.*, *29*, 1449–1462.

Roncoli, C., K. Ingram, and P. Kirshen (2002), Reading the rains: Local knowledge and rainfall forecasting in Burkina Faso, *Soc. Nat. Res.*, *15*, 409–427.

Saha, S., and P. Tripp (2013), The CFSv2 Retrospective Forecasts. [Available at http://cfs.ncep.noaa.gov/cfsv2/ docs.html.]

Saha, S., et al. (2006), The NCEP Climate Forecast System, *J. Clim.*, *19*, 3483–3517.

Saha, S., et al. (2013), The NCEP Climate Forecast System version 2, *J. Clim.*, *27*, 2185–2208, doi:10.1175/JCLI-D-12-00823.1.

Salzmann, U., and P. Hoelzmann (2005), The Dahomey Gap: An abrupt climatically induced rain forest fragmentation in West Africa during the late Holocene, *Holocene*, *15*(2), 190–199.

Schneider, U., A. Becker, P. Finger, A. Meyer-Christoffer, B. Rudolf, and M. Ziese (2011), *GPCC Full Data Reanalysis Version 6.0 at 0.5°: Monthly Land-Surface Precipitation From Rain-Gauges Built on GTS-Based and Historic Data*, Global Precip. Climatol. Cent., Deutscher Wetterdienst, Germany.

Shanahan, T., et al. (2009), Atlantic forcing of persistent drought in West Africa, *Science*, *324*, 377–380.

Sheffield, J., et al. (2014), A drought monitoring and forecasting system for sub-Sahara African water resources and food security, *Bull. Am. Meteorol. Soc.*, *95*, 861–882.

Skamarock, W., J. B. Klemp, J. Dudhia, D. O. Gill, D. Barker, M. G. Duda, X.-Y. Huang, W. Wang, and J. G. Powers (2008), A description of the advanced research WRF version 3, *NCAR Tech. Note NCAR/TN-475+STR*, NCAR, Boulder, Colo.

Steiner, A., J. Pal, S. Rauscher, J. Bell, N. Diffenbaugh, A. Boone, L. Sloan, and F. Giorgi (2009), Land surface coupling in regional climate simulations of the West African monsoon, *Clim. Dyn.*, *33*, 869–892.

Stockdale, T., et al. (2011), ECMWF seasonal forecast system 3 and its prediction of sea surface temperature, *Clim. Dyn.*, *37*, 455–471, doi:10.1007/s00382-010-0947-3.

Sylla, M., A. Gaye, J. Pal, G. Jenkins, and X. Bi (2009), High-resolution simulations of West African climate using Regional Climate Model (RegCM3) with different lateral boundary conditions, *Theor. Appl. Climatol.*, *98*, 293–314.

Sylla, M., F. Giorgi, M. Ruti, S. Calmanti, and A. Dell'Aquila (2011), The impact of deep convection on the West African summer monsoon climate: A regional climate model sensitivity study, *Q. J. R. Meteorol. Soc.*, *137*, 1417–1430, doi:10.1002/qj.853.

Tewari, M., F. Chen, W. Wang, J. Dudhia, M. A. Lemone, K. E. Mitchell, M. Ek, G. Gayno, J. W. Wegiel, and R. Cuenca (2004), Implementation and verification of the unified NOAH land surface model in the WRF model, paper presented at 20th Conference on Weather Analysis and Forecasting/16th Conference on Numerical Weather Prediction, pp. 11–15, Am. Meteorol. Soc., Seattle, Wash.

Themeßl, J., A. Gobiet, and A. Leuprecht (2011), Empirical-statistical downscaling and error correction of daily precipitation from regional climate models, *Int. J. Climatol.*, *31*(10), 1530–1544.

Vellinga, M., A. Arribas, and R. Graham (2013), Seasonal forecasts for regional onset of the West African monsoon, *Clim. Dyn.*, *40*, 3047–3070.

von Storch, H., H. Langenberg, and F. Feser (2000), A spectral nudging technique for dynamical downscaling purposes, *Mon. Weather Rev.*, *128*, 3664–3673.

Wani, S., J. Rockstroem, and T. Oweis (2009), *Rainfed Agriculture: Unlocking the Potential, Compr. Assess. of Water Manage. in Agric. Ser.*, CAB Int., Wallingford, U. K.

Wilks, D. (2011), *Statistical Methods in the Atmospheric Sciences*, Academic Press, San Diego, Calif.

Wilks, D., and C. Godfrey (2002), Diagnostic verification of the IRI net assessment forecasts, 1997–2000, *J. Clim.*, *15*, 1369–1377.

Xue, Y., M. Chen, A. Kumar, Z. Hu, and W. Wang (2013), Prediction skill and bias of tropical Pacific sea surface temperatures in the NCEP Climate Forecast System version 2, *J. Clim.*, *26*, 5358–5378.

Yuan, X., E. Wood, L. Luo, and M. Pan (2011), A first look at Climate Forecast System version 2 (CFSv2) for hydrological seasonal prediction, *Geophys. Res. Lett.*, *38*, L13402, doi:10.1029/2011GL047792.

Yuan, X., E. Wood, N. Chaney, J. Sheffield, J. Kam, M. Liang, and K. Guan (2013a), Probabilistic seasonal forecasting of African drought by dynamical model, *J. Hydrometeorol.*, *14*, 1706–1720.

Yuan, X., E. Wood, J. Roundy, and M. Pan (2013b), CFSv2-based seasonal hydroclimatic forecasts over the conterminous United States, *J. Clim.*, *26*, 4828–4847.

Ziese, M., A. Becker, P. Finger, A. Meyer-Christoffer, B. Rudolf, and U. Schneider (2011), GPCC first guess product at 1.0 degree: Near real-time first guess monthly land-surface precipitation from rain-gauges based on SYNOP data, doi:10.5676/DWD_GPCC/FG_M_100.

Zuo, Z., S. Yang, Z. Hu, D. Zhang, W. Wang, B. Huang, and B. Wang (2013), Predictable patterns and predictive skills of monsoon precipitation in Northern Hemisphere summer in NCEP CFSv2 reforecasts, *Clim. Dyn.*, *40*, 3071–3088.